The University of Kansas

Information and
Telecommunication
Technology Center

RAPIDLY DEPLOYABLE RADIO NETWORK

ARPA ORDER NUMBER. 8195
FBI Contract Number J-FBI-94-223

FINAL REPORT

December 31, 1997

ITTC-FY98-TR-10920-28

Principal Investigator: K. Sam Shanmugan

Co Investigators: Gary Minden, Victor S. Frost, Joseph B. Evans, Glenn Prescott, Richard Plumb, David Petr, and James Roberts

Table of Contents

EXECUTIVE SUMMARY

Objective: The primary objective of the Rapidly Deployable Radio Network project is to create architectures, protocols, and prototype hardware and software for a high speed network that can be deployed rapidly in areas of military conflicts or civilian disasters where communication infrastructures are lacking and/or destroyed (e.g. Desert Storm, Bosnia, Hurricane Andrews, LA earthquake).

Approach: The rapid deployment requirement coupled with higher speed requirements and seamless integration with other commercial networks has lead to an approach that uses wireless technology for the communication links and ATM for networking. The Rapidly Deployable Radio Network (RDRN) architecture developed by the University of Kansas is a wireless ATM network and it consists of portable (mobile) communication nodes which can be deployed on the ground or on mobile platforms such as trucks, helicopters or fixed wing aircraft. When deployed, the nodes use GPS derived location information to automatically configure themselves into a high capacity, fault tolerant network infrastructure.

Figure 1. Rapidly Deployable Radio Network

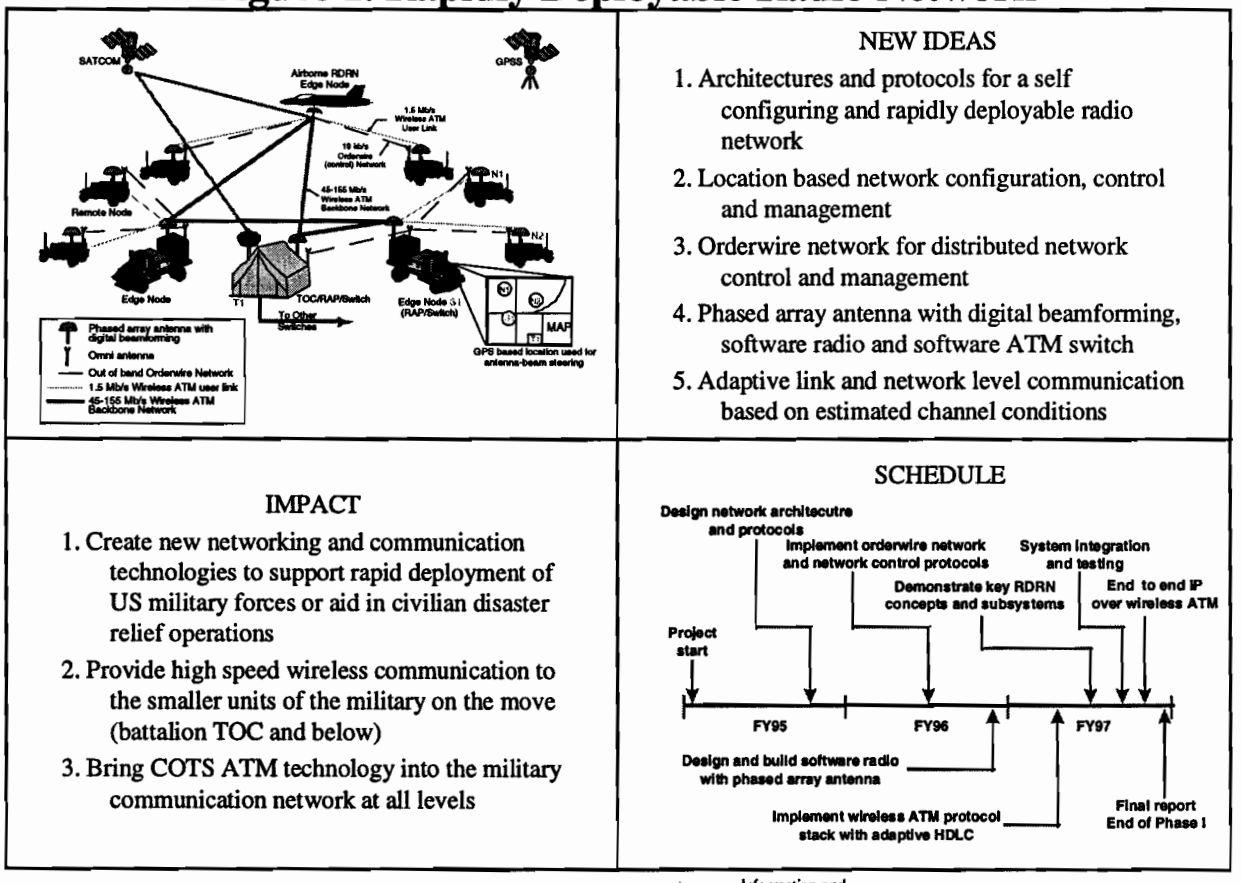

University of Kansas Information and Telecommunication Technology Center

RDRN is made up of two types of nodes: end user remote nodes (RN) providing wireless ATM access for users at a rate of up to 1.5 Mbit/s and edge nodes (EN) which serve as Radio Access Points (RAPs) or base stations and provide switching and connectivity between users. Both types of nodes contain 1) GPS receivers for location determination, 2) software controlled radios with phased-array antennas for beam forming and pointing in the right direction using GPS derived location information, and 3) Network Control (NC) software. The edge nodes also have integral ATM (software) switches and they may be interconnected by high capacity (45 to 155 Mbit/s) directional radio links. Edge nodes can also interface to wired ATM networks.

The RDRN architecture consists of three overlaid radio networks (See Figure 1): 1) a low bandwidth, low power, omni-directional order wire packet radio network for broadcasting location information, network configuration and management; (2) a cellular like ATM radio network for end user access to edge nodes with hand-offs, and (3) a high capacity wireless ATM back bone network providing connection between switches using high capacity radios with multiple directional beams.

When RDRN is initially deployed in a new area, each of the edge nodes initiate the following activities: (l) determine its location from GPS and broadcast it over the secure orderwire network; (2) listen for broadcasts from other nodes; (3) establish the backbone network by forming high capacity, directional radio links to nearby nodes using the steerable phased array antenna; and (4) begin executing the distributed network configuration and control algorithm and establish connectivity with end user nodes.

Each edge node is capable of forming multiple radio beams in the direction of other edge nodes or towards end users in the vicinity. A phased array antenna with digital beam forming is used to form these multiple beams, and pointing directions are derived from location information. Assignment of beams to users, node to node connections, and handoffs of users from one edge node to another are controlled by the distributed network configuration and management algorithm. The network control information is broadcast over the orderwire network. Changes in network topology due to mobility or failure of nodes and or links are detected by the network control algorithms and reconfiguration is carried out automatically in a distributed manner.

RDRN is also adaptable to changes in the quality of the radio communication environment. While ATM is designed to operate on high quality (almost error free) wired links, typical radio links suffer higher error rates and the link quality changes as a function of time due to mobility and changes in the environment. By estimating the channel parameters such as multipath spread and signal to noise ratio, communication parameters at the link and network levels are adapted to provide appropriate throughput and quality of service.

Project Accomplishments: Prototype algorithms, hardware and software have been developed to demonstrate the following key concepts of RDRN: (1) software controlled radio, (2) phased array antenna with digital beamforming, (3) orderwire system for network configuration and control, (4) protocol stack(s) for wireless ATM and IP over ATM and (5) Mini- ATM (software) switch. All the major subsystems of RDRN were demonstrated in the laboratory including: the

orderwire network, location-based network control algorithms, protocol stack for IP over wireless ATM, digital beamforming antenna array, and mini-ATM (software) switch. The software controlled radio with the adaptive antenna array was tested over a 10 km link at a rate of 1 Mb/s and the link budget was verified. The adaptive HDLC protocol stack for transmitting multiple ATM cells per HDLC frame over the wireless link was simulated and the optimum frame size as a function of link quality using simulations. Interoperability of RDRN with other wired and wireless systems were demonstrated during the July '97 GLOMO principal investigators meeting at Fort Monmouth, NJ.

Many of the RDRN concepts developed thus far have been explored for commercial and military applications through active involvement with Sprint Corporation (Overland Park, Kansas) and the Radio Access Point program (US ARMY CECOM, Fort Monmouth)

This report *summarizes* the accomplishments of the RDRN Phase I program. The contents of the report are organized into four sections, beginning with a detailed description of the RDRN architecture and protocols followed by Section 2 which provides an overview of the RDRN prototype transmitter/receiver system and interface. Section 3 of the report contains a brief description of the antenna arrays and the link budget for RDRN radio links is provided in Section 4. The last section of the report describes the results of system level and interoperability tests and demonstrations. Each section of the report contains additional references including a list of detailed and relevant technical reports and additional information available to the interested reader. (Please refer to the website http://www.ittc.ukans.edu/RDRN/ for on-line information on RDRN.)

1. RDRN NETWORK ARCHITECTURE AND PROTOCOLS

1.1 Introduction

This chapter provides a summary of the network architecture, configuration and control algorithms, and the link protocols for the Rapidly Deployable Radio Network (RDRN). The objective of the developed architecture was to use adaptive point-to-point topology to gain the advantages of ATM for wireless networks. The architecture is composed of three overlaid networks: (1) a low bandwidth, low power omni-directional network for location determination, switch coordination and management; (2) a "cellular like" system with adaptive directional antennas for multiple end-user access to a switch; and (3) a high capacity, highly directional, multiple beam network for switch-to-switch communication. The architecture developed here supports virtual circuits based on Broadband Integrated Services Digital Network (B-ISDN) concepts, in particular, the ATM protocols. Thus, all network element are compatible with the evolving telecommunications infrastructure. The use of end-to-end and standards-based ATM technology allows for the seamless integration of this wireless network into existing systems and the subsequent potential for scaling into a large system.

A prototype of the RDRN system has been implemented and the key concepts have been demonstrated using the testbed built around the prototype RDRN system. An overview of the The prototype RDRN system and the research results in the areas of configuration and control for wireless Asynchronous Transfer Mode (ATM) and the adaptive wireless link layer protocol for ATM are also presented in tis section of the report.

1.2 RDRN Phase I Architecture

The current RDRN architecture is composed of three overlaid networks:

- A low bandwidth, low power omni-directional network for location dissemination, switch coordination, and management which is the orderwire network.
- A "cellular-like" system for multiple end-user access to the switch using directional antennas for spatial reuse, and a high capacity, highly directional, multiple beam network for switch-to-switch communication.
- A high capacity wireless ATM backbone network that connects the switching nodes.

The network currently consists of two types of nodes, Edge Node (EN)s and Remote Node (RN)s as shown in Figure 1.1. ENs were designed to reside on the edge of a wired network and provide access to the wireless network; however, ENs also have wireless links. The EN components include Edge Switch (ES)s and optionally an ATM switch, a radio handling the ATM-based communications, a packet radio for the low speed orderwire running a protocol based on X.25 (AX.25), Global Positioning System (GPS) receiver, and a processor. Host nodes or remote nodes (RN) consist of the above, but do not contain an ATM switch. The ENs and RNs also include a phased array steerable antenna. The RDRN uses position information from the GPS for steering antenna beams toward nearby nodes and nulls toward interferers, thus establishing the high capacity links as illustrated in Figure 1.2. Figure 1.2 highlights an EN (center of figure) with its omni-directional transmit and receive orderwire antenna and an omni-

directional receive and directional transmit ATM-based links. Note that two RNs share the same 45° beam from the EN and that four distinct frequencies are in use to avoid interference multiple users within a beam can also be supported by TDMA. The decision involving which beams to establish and which frequencies to use is made by the topology algorithm which is discussed later.

The EN has the capability of switching ATM cells among connected RNs or passing the cells on to an ATM switch to wire-based nodes. Note that the differences between an EN and RN are that the EN performs switching and has the capability of higher speed radio links with other Edge Switches as well as connections to wired ATM networks.

The orderwire network uses a low power, omni-directional channel, operating at 19200 bps, for signaling, control, and communicating node locations to other network elements. The orderwire aids link establishment between the ENs and between the RNs and ENs, tracking remote nodes and determining link quality. The orderwire operates over packet radios and is part of the Network Control Protocol (NCP).[1] A summary of the NCP will be given later on. An example of the user data and orderwire network topology is shown in Figure 1.3. In this Figure, an ES serves as a link between a wired and wireless network, while the remaining EN act as wireless switches.

The protocol stack for the RDRN network is shown in Figure 1.4. Figure 1.5 shows the high-speed protocol architecture on the EN while Figure 1.6 shows the corresponding architecture on the RN. As can be seen from these Figures, the differences between an EN and RN from an architecture standpoint are that the EN performs switching and has the capability of higher speed radio links with other ENs as well as connections to wired ATM networks. In Figure 1.5, the ATM-based MicroSwitch driver performs cell switching in software.

Linux has been chosen as the operating environment for the RDRN system. The system supports applications running over both native-mode ATM as well as TCP/IP over ATM. There has been considerable development work done to support standard ATM on Linux by researchers at the Laboratoire de Reseaux de Communication (LRC) at EPFL in Switzerland [1]. In particular, they have developed a BSD-sockets based application programming interface (API) to support native-mode ATM applications as well as support for classical IP over ATM (RFC 1577) for TCP/IP based ATM applications [2]. The Device-independent ATM coordination layer shown in Figures 1.5 and 1.6 is a collection of common data structures and protocol

[1] The Simple Network Management Protocol (SNMP) Management Information Base (MIB) for the NCP operation as well as live data from the running prototype RDRN system can be retrieved from http://www.ittc.ukans.edu/~sbush/rdrn/ncp.html.

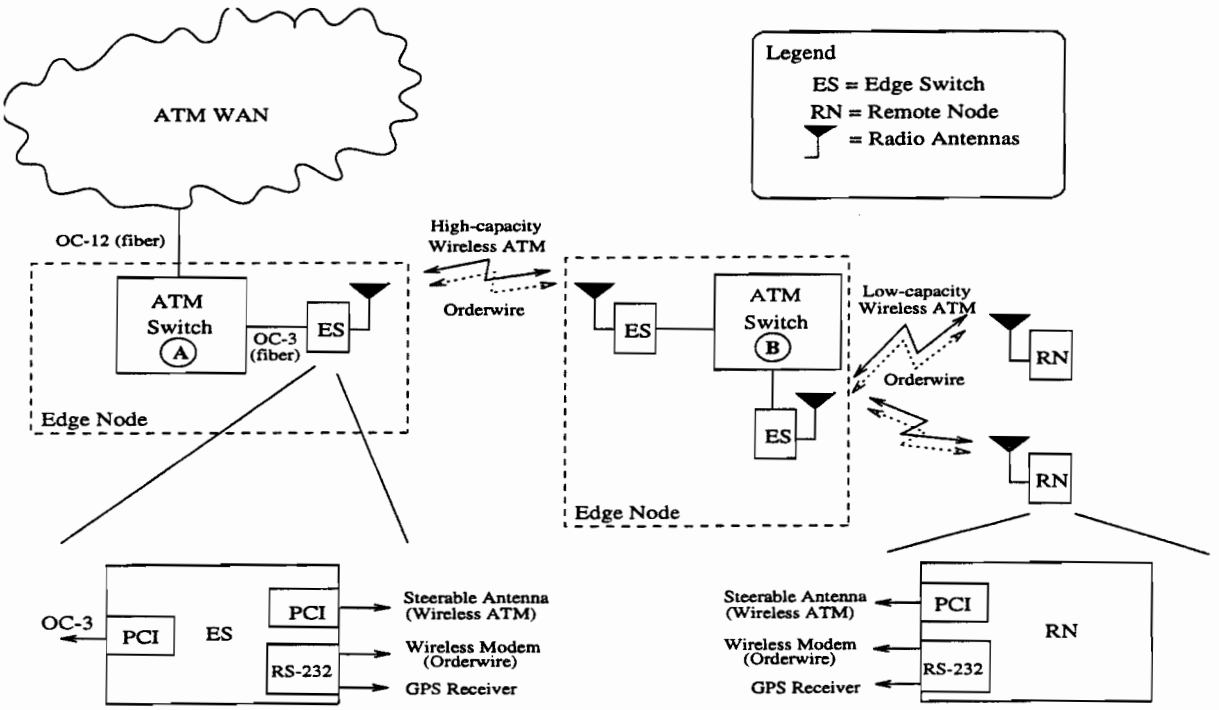

Figure 1.1: RDRN High-Level Architecture

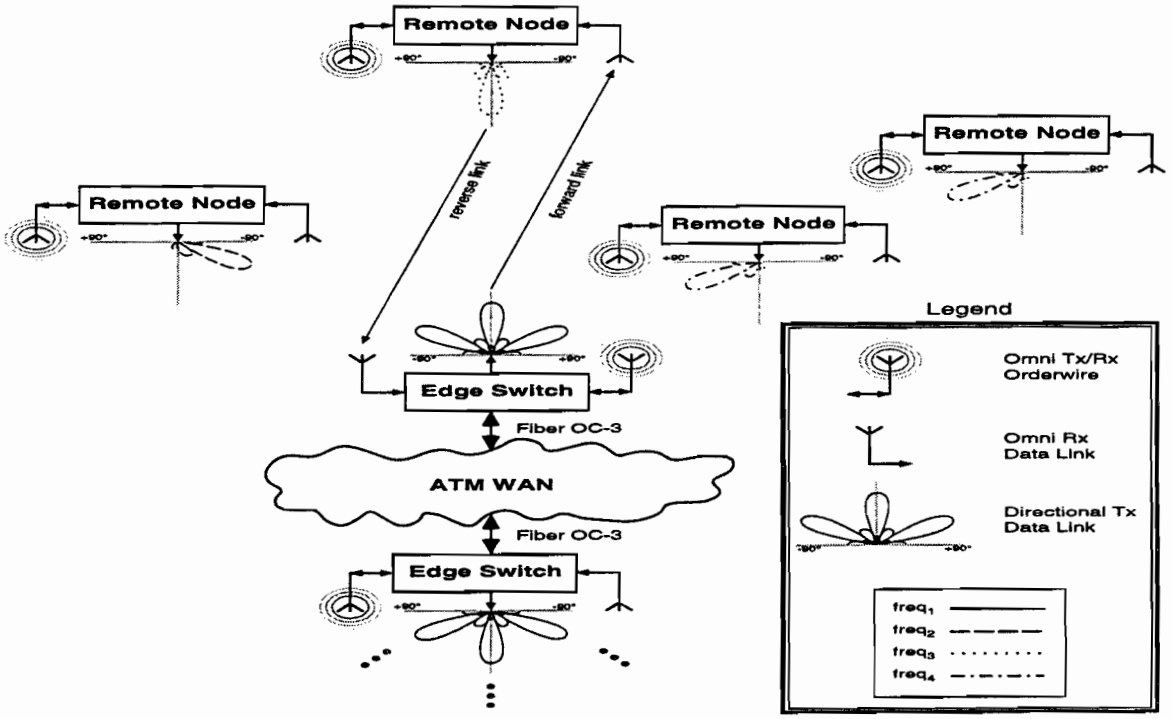

Figure 1.2: RDRN Component Overview

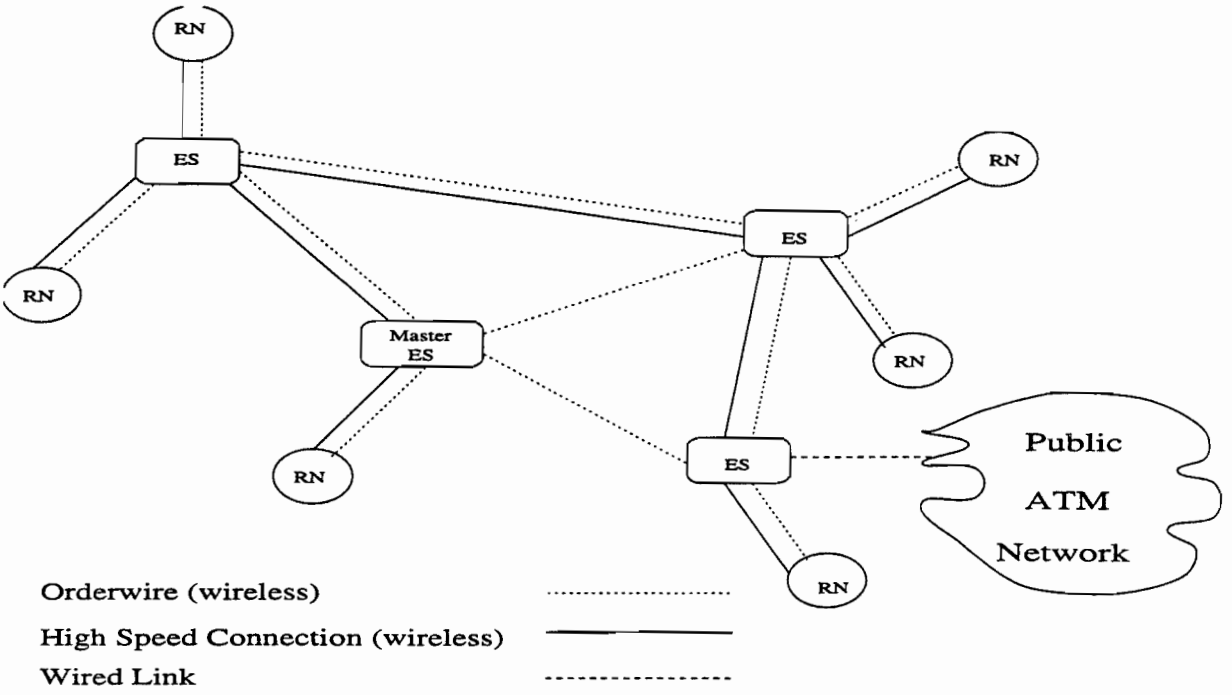

Figure 1.3: Example Orderwire Topology

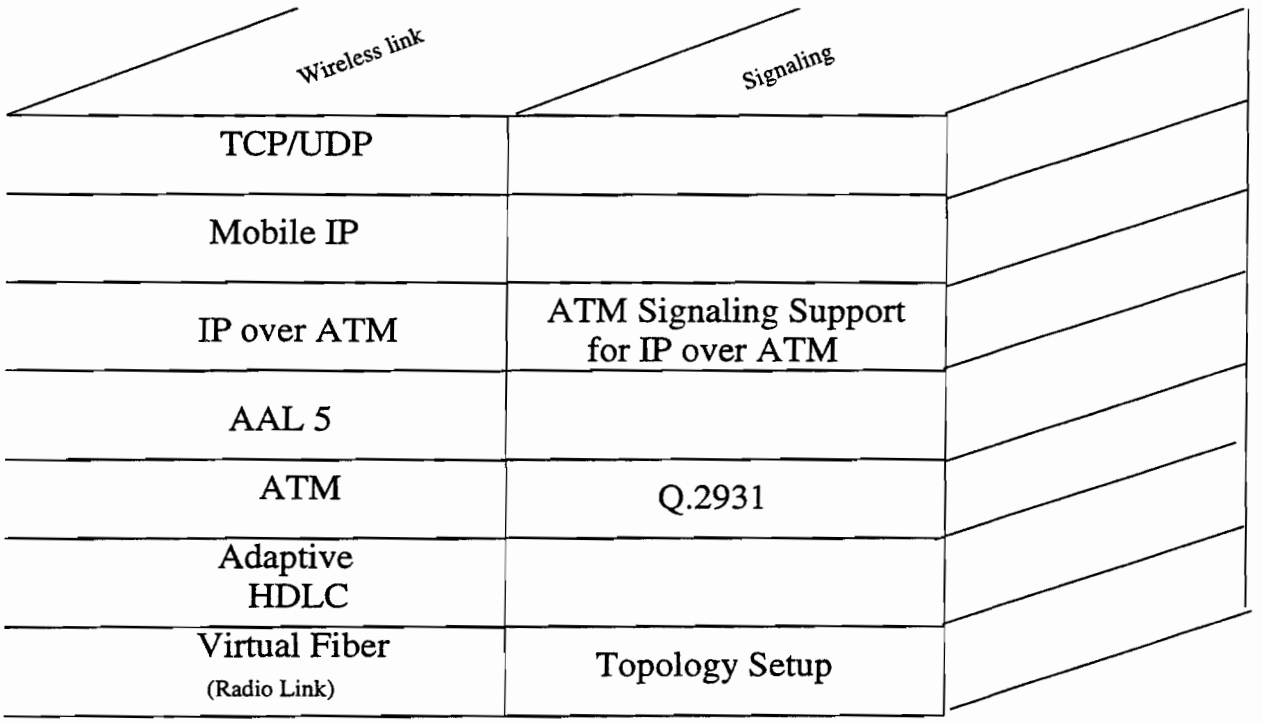

Figure 1.4: Wireless ATM Protocol Stack

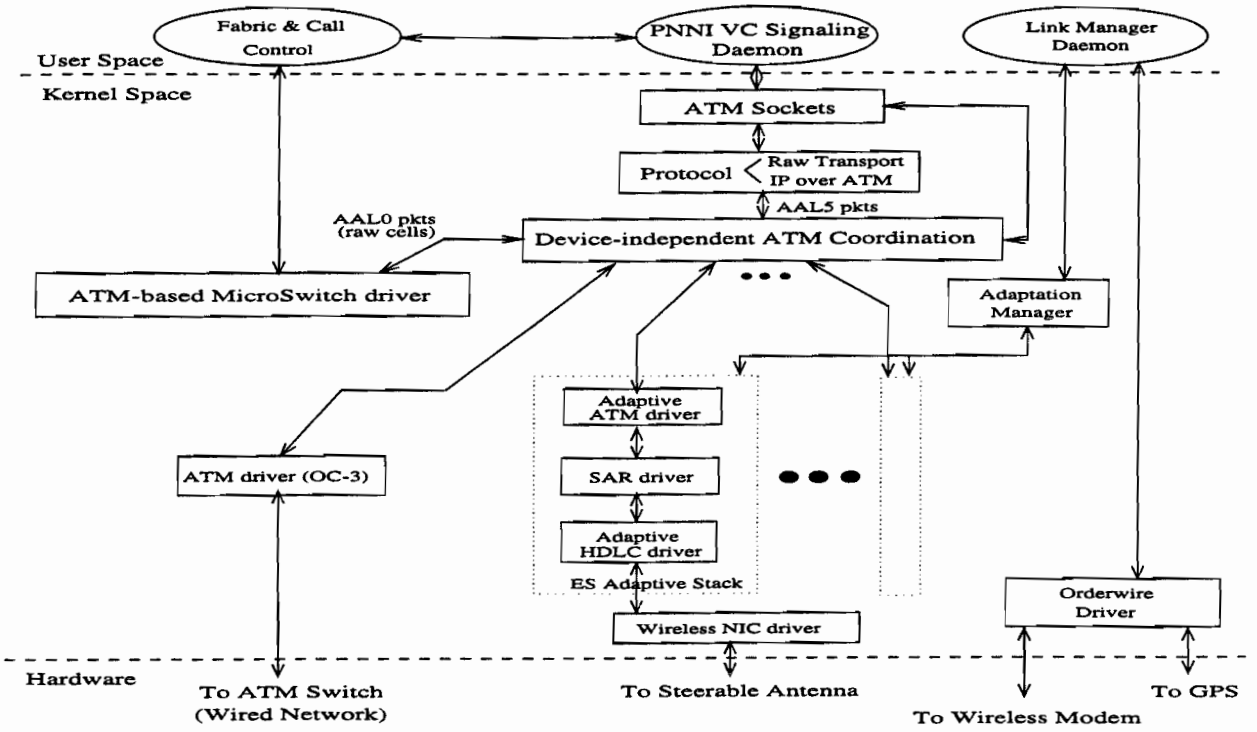

Figure 1.5: EN Network Architecture

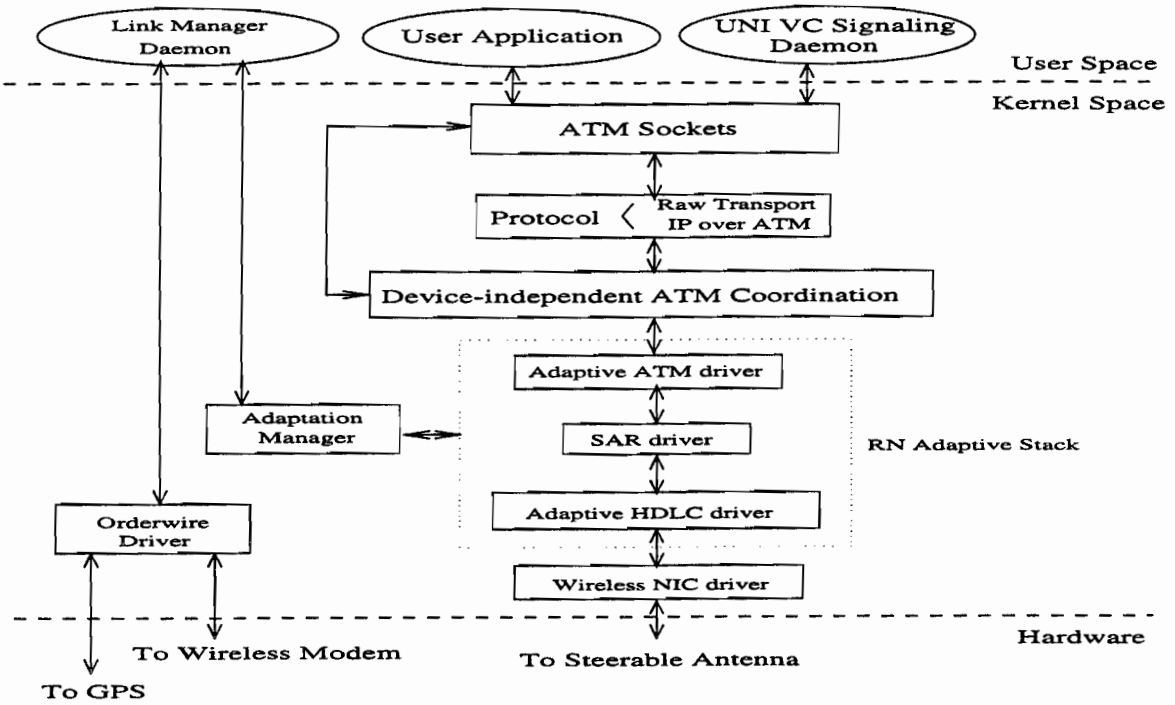

Figure 1.6: RN Network Architecture

conventions for ATM on Linux. The available software from the ATM on Linux distribution has been reused in the RDRN system. Thus the wireless ATM software stack developed for the RDRN system can be treated just like any other ATM device driver and interfaces into the standard distribution at the Device-independent ATM Coordination layer as shown in Figures 1.5 and 1.6. The wireless ATM software stack for RDRN consists of an adaptive ATM layer, a segmentation and reassembly layer (SAR), an adaptive data link layer and a wireless ATM interface layer.

A goal of the design was to keep the wireless components as simple as possible. It would be attached to an existing ATM switch through a single port, creating a node which could reside at the edge between a fixed and wireless network. However, well known VCs such as 1 (GSMP) 5 (Q.2931), and 16 (SNMP) would overlap for all remote hosts. It was decided to incorporate ATM switching into the wired/wireless nodes, thus eliminating the need for an offboard ATM switch. Because the interface has switching capability, overlapping VC space is not a problem and RN to RN connections at the same Edge Node (base station) can be connected directly together without having to go through an off-board ATM switch. A disadvantage of incorporating ATM switching into the wireless interface is that some extra features incorporated in commercial ATM switches, such as topology acquisition, LAN Emulation, switching agent, etc. will not be available without significant additional development effort.

The protocol on the EN will remove ATM cells form the HDLC-like frames and switch the cells to the proper port. It will also pack ATM cells into an HDLC-like frame to send to the radio. Figure 1.7 shows the Linux environment on the RN. The ATM Device Driver API and HDLC-like Driver are detailed in Figures 1.6 and 1.7.

A detailed view of the software architecture for the EN is shown in Figure 1.8. There is one Packet Radio driver for the antenna with multiple EN Adaptive drivers, one per RN. The ATM Microswitch is shown in the middle of the EN. The Microswitch performs software ATM cell switching. Note that an EN connecting a wireless EN-EN will only have a single EN Adaptive driver and will contain a special version of the ATM Microswitch which will simply pass through ATM cells. In this case the EN-EN link would require a directly connected ATM switch.

1.3. RDRN Protocol Layers

The protocol layers used in RDRN will provide the framework for summarizing the contributions of the research.

1.3.1 Physical Layer

The physical layer includes all hardware components and the wireless connections. This includes the high speed radios, orderwire packet radios, ATM switch, antennas, and additional processor for configuration and setup. This layer provides a raw pipe for the data link.

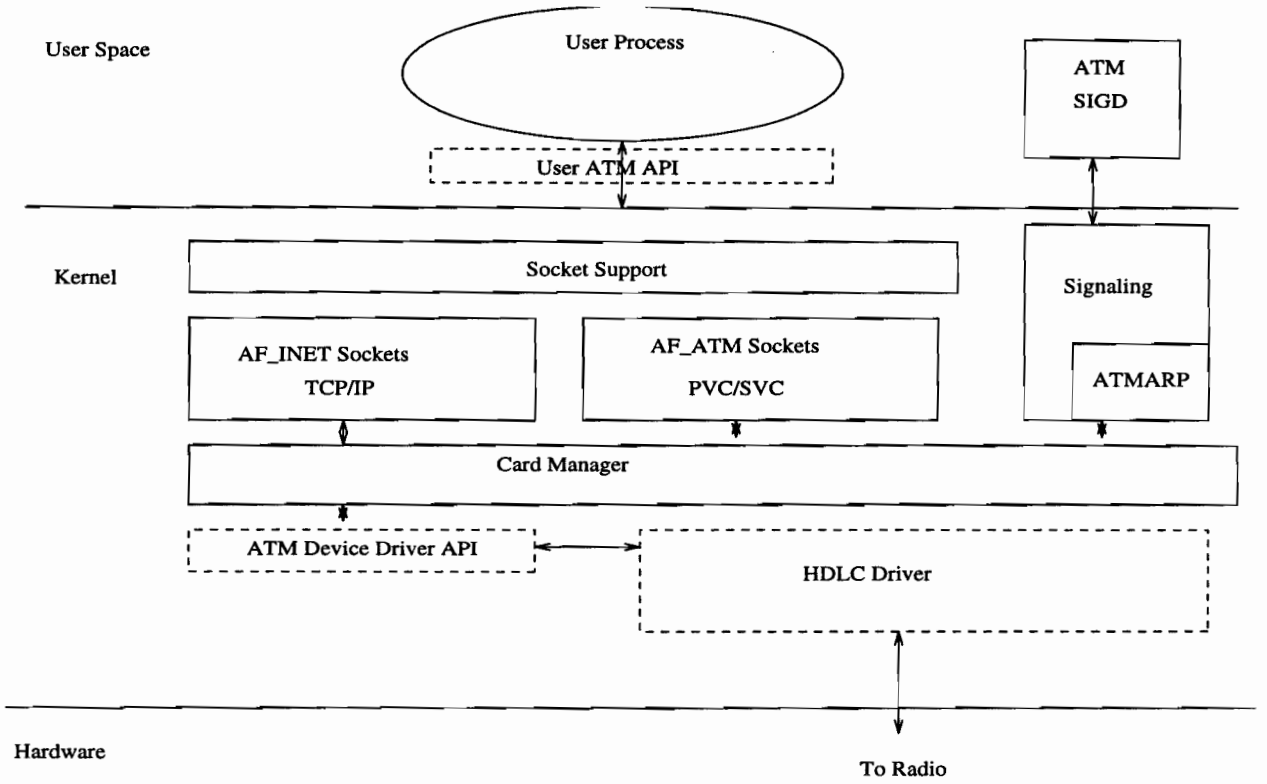

Figure 1.7: RN Linux ATM Protocol Stack

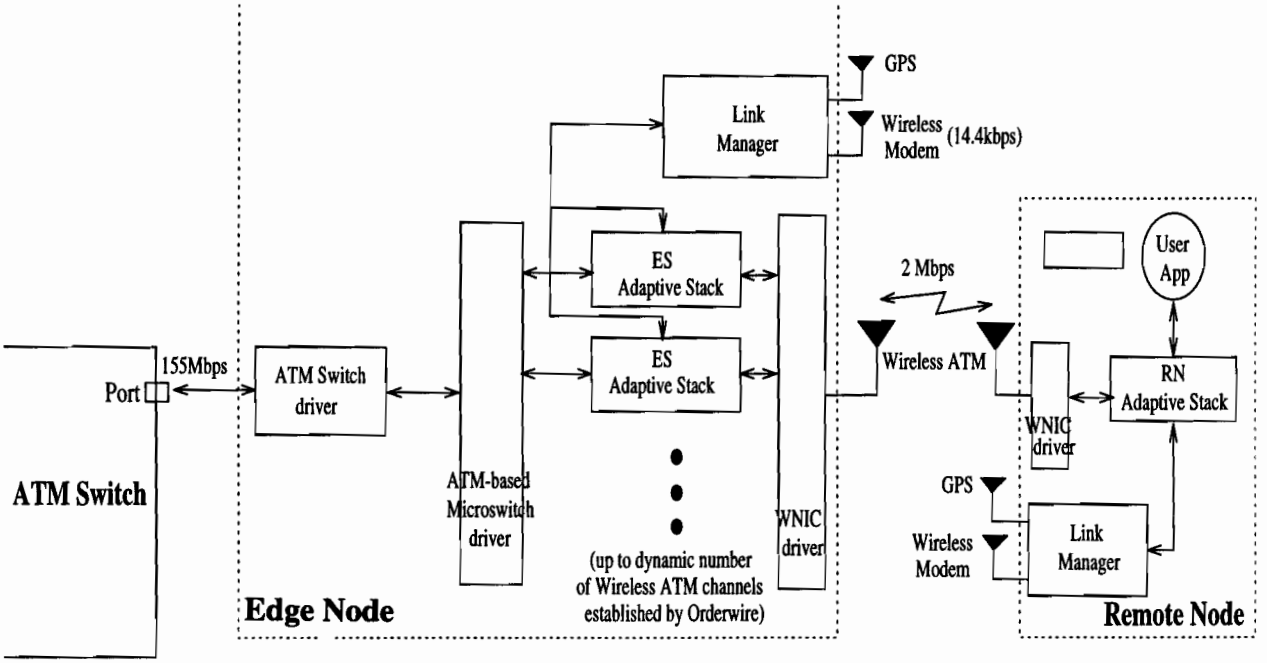

Figure 1.8: Detailed View of Edge Node Connection to Remote Node

Directional beams from a single antenna are used to obtain spatial reuse and Time Division Multiple Access (TDMA) is used to provide access to multiple RNs within a beam. The physical layer details can be found in [3]. The RDRN architecture deals with several aspects of the physical layer.

A novel algorithm has been developed to associate ENs to RNs, i.e., the algorithm determines a physical topology between an edge node and its remote nodes. The topology is formed based on:

1. The assignment or mapping of radio beams to remote nodes. This assignment is edge node's server map.
2. The number of radio beams to form.
3. The direction or steering angle of each beam.
4. The relative power of each beam.

The RDRN makes these decisions to maximize the minimum signal-to-interference ratio of the remote nodes.

After the topology has been found the newly developed Network Control Protocol (NCP) sets up the physical layer wireless connections. The NCP Architecture is shown in Figure 1.9. At the physical level the orderwire exchanges position, time and link quality information and to setup the wireless connections. The network will have one Master EN, which will run the topology configuration algorithm [4] and distribute the resulting topology information to all the connected ENs over point-to-point orderwire packet radio links using the NCP. In the current prototype the point-to-point link layer for the orderwire uses AX.25 [5]. The Master EN is initially the first active EN, and any EN has the capability of playing the role of the Master.

In order to make RDRN truly rapidly deployable, configuration at all layers has to be a dynamic and continuous process. Configuration can be a function of such factors as load, distance, capacity and permissible topology, all of which are constantly changing in a mobile environment. A Time Warp [6] based algorithm is used to anticipate configuration changes and speed the reconfiguration process. The Virtual Network Configuration (VNC) algorithm is an application of a more general mechanism called Time Warp Emulation (TWE). Time Warp Emulation is a modification of Time Warp [6]. The motivation behind TWE is to allow the actual components of a real-time system to work ahead in time in order to predict future behavior and adjust themselves when that behavior does not match reality. This is accomplished by realizing that there are now two types of messages, those which arrive in the past relative to the process's Local Virtual Time (LVT) and those messages which have been generated which are time-stamped with the current real time, but whose values exceed some tolerance from the component's current value. The basic Time Warp mechanism is modified by adding a verification query phase. This phase occurs when real time matches the receive time of a message in the output queue of a process. In this phase, the physical device being emulated in time is queried and the results compared with the value of the message. A value exceeding a prespecified tolerance will cause a rollback of the process. Application of the VNC algorithm to RDRN can be explained by an example. A remote node's direction, velocity, bandwidth used, number of

connections, past history and other factors can be used to approximate a new configuration sometime into the future. All actual configuration processes can begin to work ahead in time to where the remote node is expected to be at some point in the future. If the prediction is incorrect, but not far off, only some processing will have to be rolled back in time. For example, the algorithm to determine the physical topology may have to be adjusted, but the resulting topology and many higher level requirements will still be correct. Working ahead and rolling back to adjust for error with reality is an on-going process, which depends on the tradeoff between allowable risk and amount of processing time allowed into the future. Figure 1.10 illustrates that VNC can speed up the configuration process by factors of 2 to 3. The VNC speed up is a function of the number of out-of-tolerance messages. An out-of-tolerance message indicates that the prediction exhibits enough error to cause a rollback. A large proportion of out-of-tolerance messages will, in theory, cause the process to do additional processing beyond that required of a non-VNC system, reducing the speed up below one. Details of the VNC algorithm and its analysis can be found in [10].

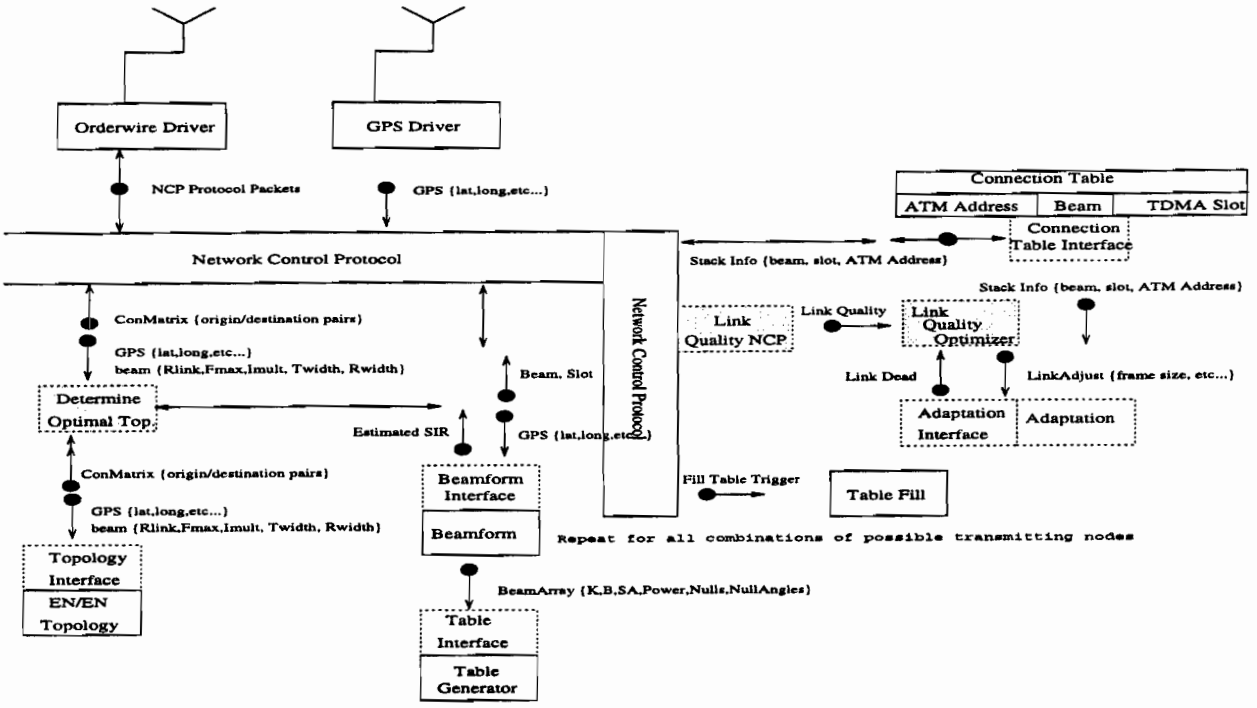

Figure 1.9: Network Control System Architecture

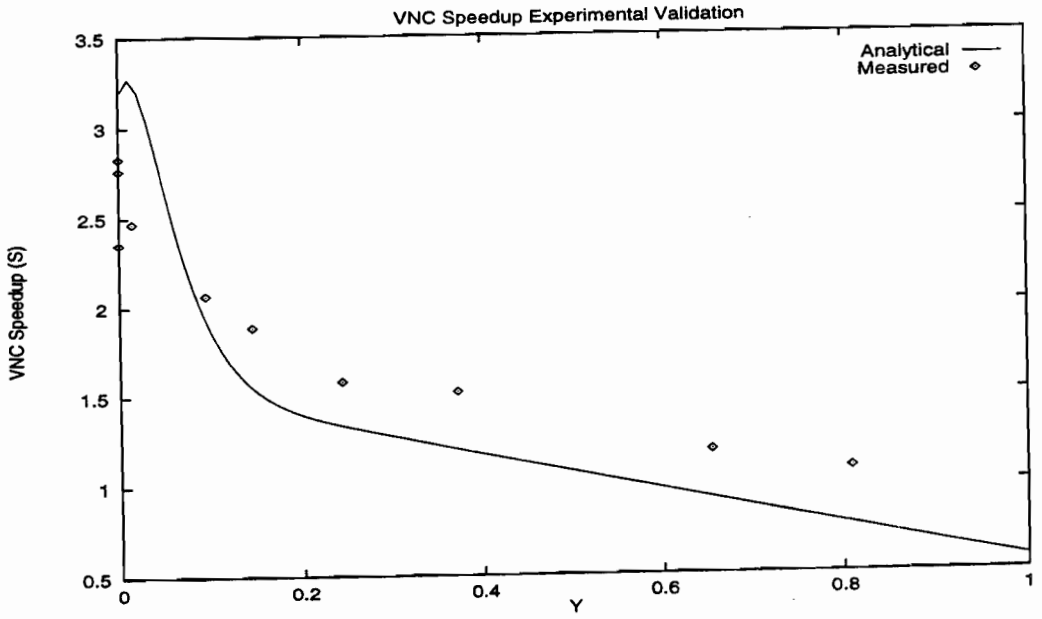

Figure 1.10: EN Beam Creation Speedup

1.3.2 Link Layer

In the RDRN architecture ATM is carried end-to-end. However, at the edge between the wired (high-speed) network and wireless links, multiple ATM cells are combined into an HDLC-like frame. These frames comprise the adaptive HDLC (AHDLC) protocol. The wireless data link layer for RDRN is adaptive to provide an appropriate trade-off between data rate and reliability in order to support the various services. For example, time sensitive voice packets may be dropped, but data packets will be retransmitted. The edge interface unit makes this decision based on knowledge of the requirements of each traffic stream, possibly based on virtual circuit number.

For some types of traffic, error correction may be achieved using retransmission. Here, delay is increased for this class of traffic to prevent cell losses. It is well known that even a few cell losses can have a significant impact on the performance of TCP/IP (Transmission Control Protocol/Internet Protocol), while TCP/IP can cope with variable delay [7]. AHDLC protocol can change in response to traffic requirements. Specifically, the wireless channel state is estimated based on the ratio of the number of frames received with and without errors and is assumed to be in either a good state (characterized by a low BER) or a bad state (characterized by a high BER). The wireless frame length is then adapted to the channel state with a larger frame used in the good state and a smaller one in the bad state. An *n-copy* mechanism is also used (either alone or in combination with the adaptive frame length algorithm). Here in the bad state multiple copies of each delay-insensitive traffic frame are transmitted in order to reduce the total number of retransmission requests. The adaptive protocol attempts to maximize the throughput under all channel conditions.

The effect of using both the adaptive length and pre-emptive retrnsmission mechanisms when the channel is in the bad state have been studied. Figure 1.11 shows the variation in throughput as the error rate changes, with adaptive length and pre-emptive retransmissions with 2 copies while the plot in Figure 1.12 shows a similar variation with adaptive length and pre-emptive retransmissions with 3 copies. As we can see from Figure 1.13, combining the adaptive length with 2-copy or 3-copy schemes yields comparable performance. Thus, there is no advantage of using the 3-copy mechanism, because the loss in throughput by using the third copy is not recovered by fewer retransmissions.

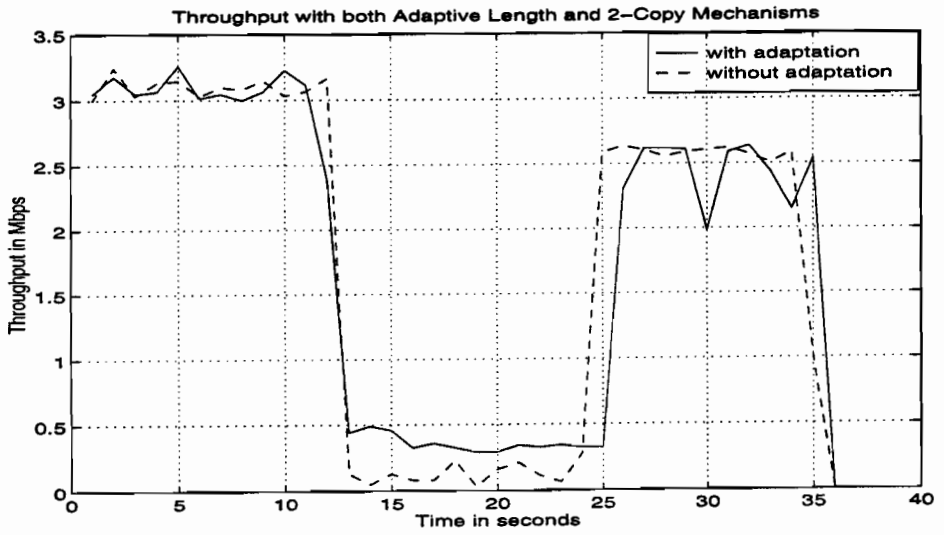

Figure 1.11: Variation of Throughput with Adaptive Length and 2-Copy Mechanisms

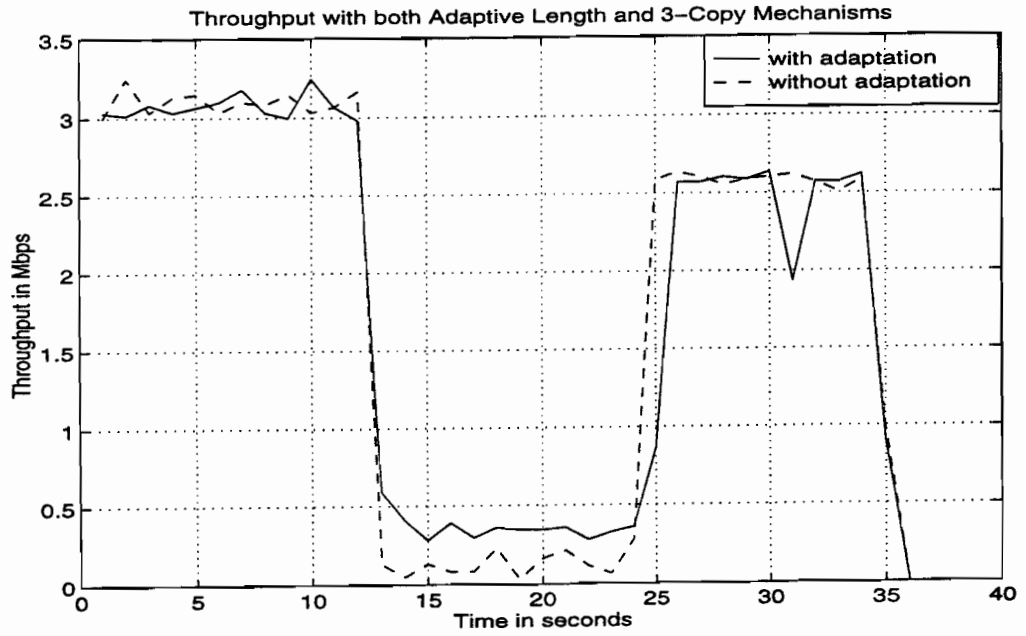

Figure 1.12: Variation of Throughput with Adaptive Length and 3-Copy Mechanisms

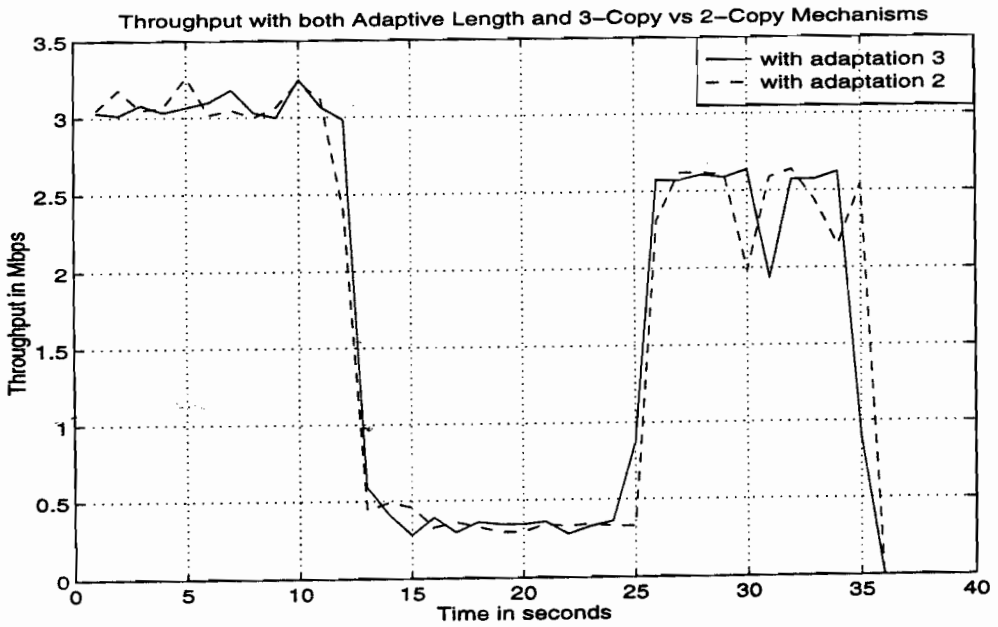

Figure 1.13: Variation of Throughput with Adaptive Length and 2-Copy vs Adaptive Length and 3-Copy Mechanisms

The link layer must also maintain cell order; this is critical during handoff of an RN from one EN to another. Figures 1.5 and 1.6 show the architecture for the link/ATM level implementation. Below the device independent ATM layer are the high peed packet radio (PR) specific layers. The RN/EN interface bridges at the cell level, not the AAL layer. No link level addressing is used since the ATM level specifies the address.

1.3.3 ATM Layer

The adaptive ATM layer provides the interface between the RDRN wireless ATM driver and the standard ATM on Linux distribution. It contains the data structures specific to the wireless ATM driver and provides the device-independent ATM coordination layer with standard device-independent entry points to the rest of the wireless software stack. It thus enables the RDRN wireless stack and the higher layers of the ATM on Linux distribution to exchange data. The adaptive ATM layer also manages resources on the wireless stack, keeps track of active VCs and gathers ATM level statistics such as cell counts, drop counts and so on. While the current implementation is non-adaptive, this layer can be enhanced to adapt the allocation and management of resources in response to certain specified parameters or events. Note that ATM protocol standards are maintained end-to-end throughout the RDRN architecture.

1.3.4 ATM SAR Layer

The SAR layer performs ATM segmentation and reassembly functions in software. The current implementation supports AAL5 and NULL (AAL0) encapsulation types. However, it must be noted that no AAL is precluded from use. The SAR layer performs one complete segmentation at a time and allows concurrent reassembly on up to 1024 VCs. For AAL5 traffic on transmit, the SAR layer receives a protocol data unit (PDU) from the device-independent ATM coordination layer through the adaptive ATM layer, performs the CRC calculations and computes the AAL5 trailer bytes. It then segments the resulting AAL5 PDU into 48 byte chunks and adds the appropriate ATM cell headers before passing the cells down to the adaptive data link control layer for transmission. For each VCI channel being reassembled, a reassembly queue is allocated in memory which is used as the workspace for the reassembly process. For AAL5 traffic, CRC calculations are performed on the reassembly queue as cells are received. AAL5 PDUs that are reassembled error-free are passed up to the device-independent layer through the adaptive ATM driver. A VCI table is used within the SAR layer to store information about all active VCs. The SAR layer employs early-packet discard to improve the efficiency of the reassembly process. The next sections discuss the network and transport layers in RDRN.

1.3.5 Network Layer

The RDRN network layer provides a well known and widely used network layer, whose primary purpose is to provide routing between subnetworks and service for the Transmission Control Protocol (TCP) and User Datagram Protocol (UDP) transport layers. The relation between IP and ATM is still an open issue. *Classical IP and Address Resolution Protocol (ARP) over ATM* [8] (CLIP) is an initial standard solution. However, it has several weak points such as requiring a router to connect Logical IP Subnet (LIS) even when they are directly connected at the ATM level, and requiring an Asynchronous Transfer Mode Address Resolution Protocol (ATMARP) server to provide address resolution for a single LIS. *The Non-Broadcast Multiple Access (NBMA) Next Hop Resolution Protocol (NHRP)* [9] provides a better solution but it is still in draft form. The RDRN architecture has implemented CLIP and supports both PVCs and SVCs via ATMARP.

1.3.6 Transport Layer

This section focuses on the effects of mobility on the transport layer. The transport layer provides end-to-end connectivity. Note that the UDP/IP service allows dropped or unordered packets, while the TCP/IP service guarantees packet delivery. An open issue concerns whether TCP should be terminated at the EN on the fixed network side, allowing for a modified and more robust protocol across the wireless link. Initially, TCP/IP will not be terminated at the EN, but continue end-to-end. However, the adaptive link layer protocol in RDRN effectively hides wireless link errors from TCP.

Because of congestion control, current TCP implementations may suffer unacceptable delays during handoffs [7]. The handoff delay will cause the TCP window size to drop, a slow start algorithm will begin, and the retransmission timer will be set to a back-off interval that

doubles with each consecutive timeout. The result is much larger drop in throughput and delay than simply the time required to handoff. The Virtual Network Configuration (VNC) Algorithm [10], previously discussed in [11], provides a solution to this problem. Because the network configuration system runs ahead of real time, throughput should be as least as good as that shown for overlapping cells in [7]. A solution to help ease congestion of TCP/IP over ATM is given in [12].

1.3.7 Application Layer

RDRN can transport any native ATM or TCP/IP application. The prototype system was demonstrated using internet video, audio, and whiteboard applications as well as standard services like, ftp and telnet.

1.4 Conclusion

The RDRN project goal was to research and prototype a high speed-ATM-based wireless communication system which is adaptive at both the link and network levels to allow for rapid deployment and response to a changing environment. RDRN involved the design and implementation of a reconfigurable ATM wireless network which uses antenna beamforming for improved spatial reuse. The objective of the architecture described here was to use adaptive point-to-point topology to gain the advantages of ATM for wireless networks. The major elements of this research were the wireless ATM protocol architecture, the configuration protocols, and the adaptive link layer protocols as summarized here.

1.5 Bibliography

[1] Werner Almesberger. *Linus ATM*, December 1995. Web Page URL: http://lrcwww.epfl.ch/kinux/atm/.

[2] Werner Almesberger. *Linus ATM API*, July 1996. Web Page URL: http://lrcwww.epfl.ch/kinux/atm/.

[3] Benjamin Ewy, Craig Sparks, and K. Sam Shanmugan. An Overview of the Rapidly Deployable Radio Network Proof of Concept System. Technical Report 10920-16, Telecommunications & Information Sciences Laboratory, July 1995.

[4] Kaushik Ghosh, Richard M. Fujimoto, and Karsten Schwan. Time Warp simulation in Time Constrained Systems. In *Proceedings of the 7th Workshop on Parallel and Distributed Simulation*, pages 163, 166, 1993.

[5] IEEE. *AX.25 Amateur Packet Radio Link-Layer Protocol*, October 1984.

[6] D. R. Jefferson and H. A. Sowizral. Fast Concurrent Simulation Using the Time Warp Mechanism, Part I: Local Control. Technical Report TR-83-204, The Rand Corporation, 1982.

[7] Ramon Caceres and Liviu Iftode. Improving the Performance of Reliable Transport Protocols in Mobile Computing Environments. *IEEE Journal on Selected Areas in Communications*, 13(5), June 1995.

[8] IETF. *Classical IP and ARP over ATM*, 1995. Online version available at http://ds.internic.net/rfc/rfc1577.txt.

[9] Routing over Large Clouds Working Group. *NBMA Next Hop Resolution Protocol (NHRP)*, 1995. Online version available at gopher://ds.internic.net/oo/internet-drafts/draft-ietf-rolc-nhrp-04.txt.

[10] Stephen F. Bush. *The Design and Analysis of Virtual Network Configuration for a Wireless Mobile ATM Network.* PhD thesis, University of Kansas, August 1997.

[11] Stephen F. Bush, Sunil Jagannath, Joseph B. Evans, and Victor Frost. A Control and Management Network for Wireless ATM Systems. In *Proceedings of the International Communications Conference '96*, pages 459, 463, June 1996. Conference wep page http://www-ee.uta.edu/organizations/commsoc/commsoft.html.

[12] Brian Buchanan. TCP/IP Header Compression for High-Speed ATM Links. Master's thesis, Telecommunications and Information Science Laboratory, University of Kansas, September 1995.

2. RDRN RADIO TRANSMITTER/RECEIVER SYSTEM AND INTERFACE

2.1 Introduction

The work presented in this section supports the effort to develop a high speed Asynchronous Transfer Mode (ATM) based wireless communication system that is adaptive at both the link and network levels to allow for rapid deployment and to respond to a changing environment. The prototype system allows mobile users called remote nodes equipped with a Global Positioning System (GPS) receiver, a packet radio system used for out-of-band orderwire signaling, and a wireless ATM interface to connect to a fiber based ATM Wide Area Network (WAN) over a re-configurable wireless ATM network. A detailed overview of the entire system can be found in Section 1 of this report and in 'Rapidly Deployable Radio Network Proof on Concept System' [1].

The RDRN system takes advantage of GPS location information to steer multiple high speed (1 to 2 Mbps) beams to mobile nodes via a multiple element phased array antenna system. In addition link quality information is also passed using the out-of-band packet radio based order wire network. This link quality information is monitored and modulation schemes, transmit frequencies, power levels, and coding schemes can be rapidly adapted to suit the changing environment. The major elements implemented in the proof of concept system are adaptive digital beamforming, an ATM based radio link, a call management and network protocol implementation, and automatic network configuration and reconfiguration.

The RDRN prototype system is a large and complex endeavor that involves the integration of many software and hardware efforts. The radio system allows multiple transmit beams to be steered to multiple mobile end users from the same antenna at the same frequency thus allowing spatial reuse of the frequency bands used. It simultaneously allows the steering angles of the beams and the modulation types used within them to adapt to a changing mobile environment. Additionally, we have investigated - but not implemented - a digital beamforming receiver. The receiver will be described later in this report.

Before the specifics of the hardware design are presented, introductory information is given that places perspective on its design. Flexible software based modulation and spatial reuse of the frequencies used are the main functions of the presented hardware therefore these topics are first introduced. The enabling technology of GPS is then discussed and shown how it makes the RDRN system possible. The out of band orderwire system is then briefly discussed.

The details of beamforming and beamsteering are then discussed and various analog and digital implementations compared and contrasted. They are followed by a description of the hardware implementation that combines the task of beamforming and flexible IF modulation into a single cost effective solution. Experimental results are then offered in support of the presented design. Finally the receiver system and the receiver digital beamforming concept is discussed.

2.1.1 Software Radio Based Flexible Modulation

Recent advances in Analog-to-Digital (A/D) converter technology has encouraged increasing interest in software controlled radio technology. With the capacity to digitize an IF or even a RF signal comes the ability to implement radio receivers that can be reprogrammed to emulate virtually any type of traditional receiver. One of the main goals of the RDRN proof of concept system is to provide a research test-bed for the development of adaptive software controlled radios. The system presented in this paper is a reprogramable transmit modulator only. The design is restricted to any type of phase or amplitude modulation. A software radio based beamforming receiver is the subject of future research.

2.1.2 Spatial Reuse

Spatial reuse of frequencies requires that the same carrier frequency must be re-used at least twice by the same transmitter within what is considered a traditional cell. This can be achieved in different ways. Figure 2.1 shows a two user scenario where the positions of the transmitting antenna labeled Edge Node and both of the Remote Nodes are all known. The steering angles for the two beams Θ_1 and Θ_2 can therefore be calculated by simple geometry.

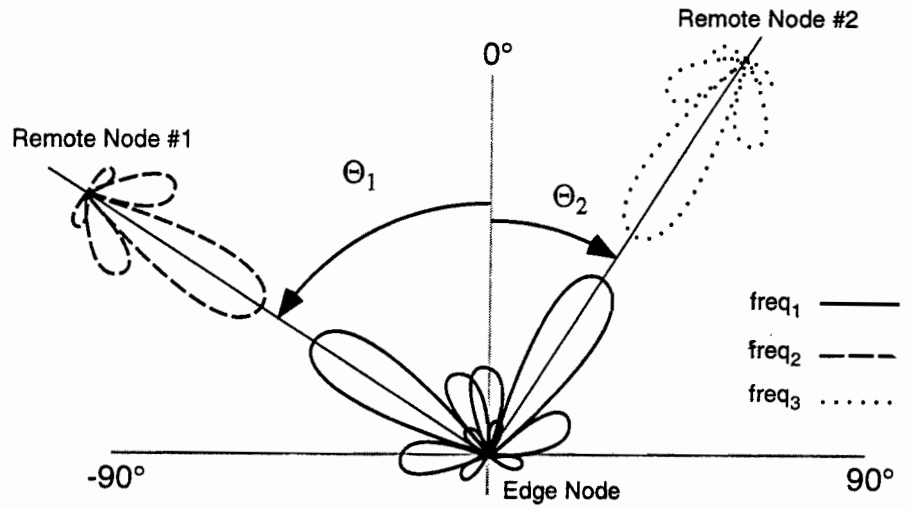

Figure 2.1: Spatial frequency reuse by beamforming.

A brute force and intuitive approach to spatial reuse of the same carrier frequency would be to use two separate microwave "dishes" both located at the transmitting Edge Node and simply point them at the individual users. This approach would work and it describes well the requirements of a system that employs spatial reuse. However it also has some serious drawbacks. The major disadvantage is that the individual beams must be steered by physically rotating the dishes to track the moving end users. In addition when the number of end users is increased the system rapidly begins to increase in both size and cost.

A better approach is the one being used in the RDRN prototype system and that is electronically controlled beamsteering in which multiple beams can be produced by a multi-element phased array antenna. The prototype systems employs in particular an equally spaced eight element linear array.

2.1.3 GPS for Position Information

Widely available and affordable GPS receivers are the enabling technology that makes the RDRN system possible. Steering beams towards mobile users requires knowledge of the physical topology of the network.

- Where is the transmitter?
- Where are the receivers with respect to the transmitter?

This information can be provided by use of GPS receivers. If every mobile user has a GPS receiver and a system can be setup to exchange this information then every node will know where every participant in the network is located.

GPS receivers provide this information in the form of latitude, longitude, and altitude. The United States Military based system does not provide non military users with the best resolution that the system has to offer. A slowly varying random variance that moves on the order of minutes is intentionally injected into the signal and can only be removed by military receivers. Fortunately the injected random variance is relatively small. It is this fact that has allowed the recent boom in commercial GPS consumer electronics. Latitude and Longitude information can be had within ±400 ft. For network nodes that are 5 miles apart this error would not pose a problem. However for nodes that are close together the limited resolution could cause difficulties.

2.2 Transmit Beamforming and Beamsteering

Several antennas can be arranged in space and interconnected to produce a directional radiation pattern. This configuration is called an antenna array, or simply, an array [3]. When the phase of the signals reaching the individual antenna elements are modified in a useful way then the antenna is called a phased array. This is the type of antenna being used in the RDRN prototype system to achieve spatial frequency reuse. The radiation pattern of an array antenna is controlled by the type of individual elements used, their orientations, their positions in space, and the amplitude and phase of the currents feeding them [3]. When the radiation pattern, called the array factor, of an antenna can be controlled in such a way as to selectively radiate energy in desired directions while simultaneously attenuating energy others this is called beamforming. Beamforming is effectively the result of farfield constructive and destructive interference patterns. A discussion of beamforming and how it applies to the RDRN prototype system follows.

2.2.1 Beamforming via Multiple Element Linear Array Antennas

An equally excited multi-element array antenna consists of N active elements that are each individually driven with the same signal. A uniformly excited, equally spaced linear array is the most simple example. It consists of N active elements lying along a line and spaced at regular intervals which are usually 1/2 wavelengths or less of their center operating frequency. Figure 2.2 is an example of a linear array and is the type used in the RDRN prototype system.

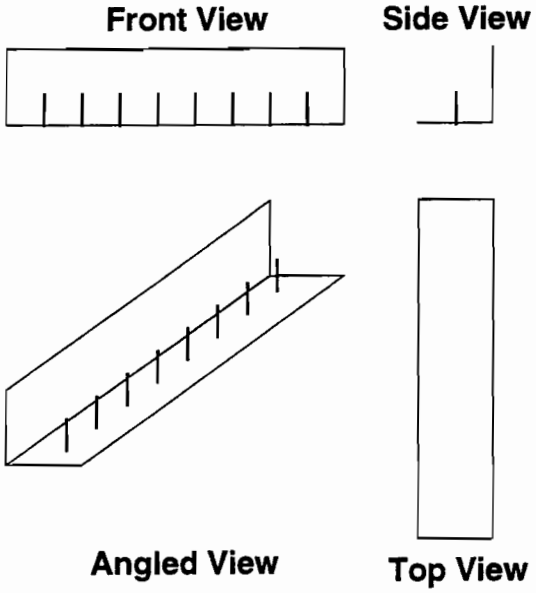

Figure 2.2: A linear array antenna.

If the eight element antenna depicted in Figure 2.2 were fed eight identical signals of equal phase and amplitude the theoretical broadside farfield pattern or array factor in Figure 2.3 would result.

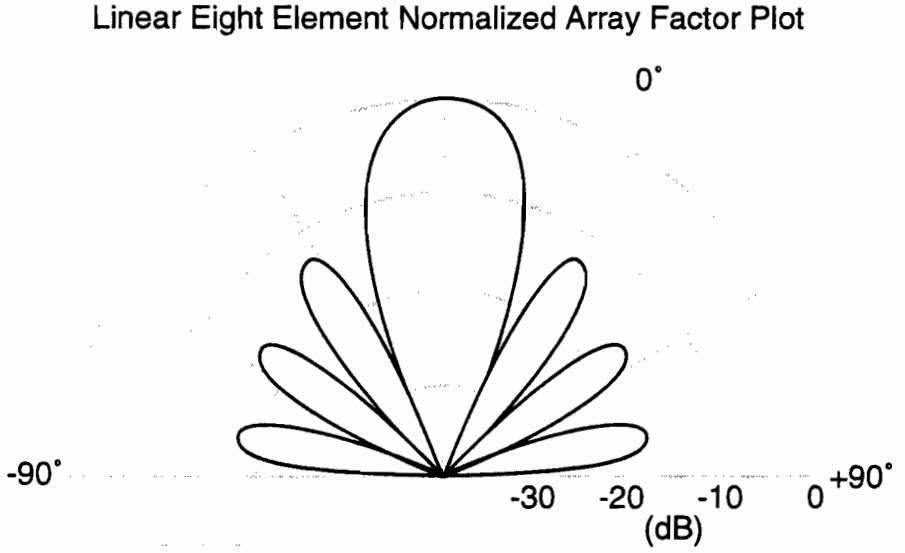

Figure 2.3: Polar array factor of an equally excited eight element linear array.

The normalized array factor appearing in Figure 2.2 is given by

$$f(\Psi) = \frac{\sin(N\Psi/2)}{N\sin(\Psi/2)} \approx \frac{\sin(N\Psi/2)}{N\Psi/2} \qquad (2\text{-}1)$$

where N is the number of antenna elements and is equal to eight and ψ is the angle off broadside [3]. It should be noted that the width of the main lobe decreases with increasing N. The reduction of the main lobe width is what allows for spatial reuse. If the width of the main lobe is made narrow enough it becomes analogous to a beam of directed energy such as a flash light. Obtaining an antenna pattern that tight would be an ideal goal. The cost involved in a large number of active antenna elements and the associated electronics needed to drive them must be weighed against the benefits of such an antenna pattern. The design goal for a multiple beam system is to find the minimum number of elements that can support the number of beams required at the desired performance or signal to interference level. For the RDRN system these cost and performance issues were balanced. The resultant tradeoff placed the number of antenna elements at eight.

2.2.2 Beamsteering by Application of Complex Weights

The broadside farfield antenna pattern shown in Figure 2.3 is only as useful as the previously mentioned microwave dish example in that it too would have to be physically pointed at the mobile user to be of any use. A linear array antenna becomes more useful when it is used as a linear phased array. By manipulating the relative phase and amplitude of the RF waveform on a per antenna element basis different interference patterns result and it is possible to rapidly "steer" a beam in a particular direction. Figure 2.4 is a block diagram representation of this process which depicts the application of N complex weights containing both phase and amplitude information to a N element array.

The weights are applied to the same RF signal on a per antenna element basis and the end effect is the ability to spatially direct the beam in a desired direction without the need to physically rotate the array. Determination of the proper complex weights needed to effect the desired amount of beamsteering is the function of beamforming and beamsteering algorithms that are detailed in the following sections.

2.2.3 Simultaneous Multiple Beams at the Same Carrier Frequency

The ability to rapidly steer a beam by electronic rather than physical means is an important advantage of a phased array antenna. There is however another and more significant advantage to the RDRN system that comes from utilizing phased array antennas. This is the ability, as previously mentioned, to use them to form multiple transmit beams to be steered to multiple mobile end users from the same antenna at the same frequency. This is spatial reuse and is one of the main goals of the RDRN proof of concept system.

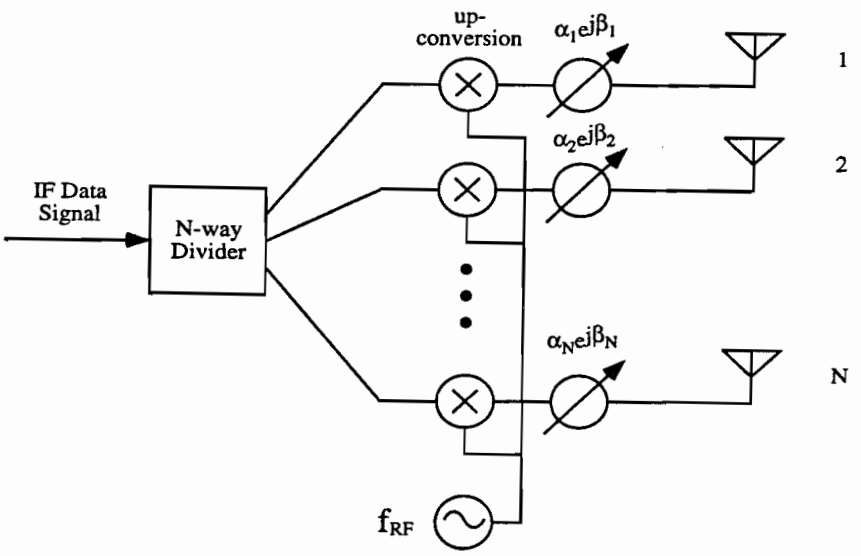

Figure 2.4: Beamsteering by the application of complex weights.

The quantity and quality, as defined by signal to interference ratio, of the multiple beams is controlled by many factors of which the number of antenna elements, their physical topology or arrangement, and the proper application of complex weights are some of the most important factors. Figure 2.5 depicts a way to form two simultaneous beams at the same frequency.

This system is the same as the single beam case appearing in Figure 2.4 with the addition of a second set of inputs. The separate inputs from the two different beamforming processes are simply summed before the antenna. The system is linear and because superposition holds for this electrical summation the output from the antenna array will the spatial sum of the individual antenna patterns. This process can be indefinitely expanded to form as many simultaneous beams as desired. There are of course some practical limits. As seen in the previous graphs of typical linear array antenna patterns sidelobes exist in the form of Sin(Nx)/Nx outputs. These sidelobes will cause interference to any other beams that are simultaneously being produced at the same frequency. Ways to reduce the level of interference include increasing the number of antenna elements, steering the beams further away from each other, and the proper application of complex weights to effect nulling patterns in the direction of other beams.

The proper application of the complex weights requires answers to at least the following questions:

- How many beams need to be formed?
- At what angles do each of the beams need to be steered?
- What is the respective relative power contained in each beam?

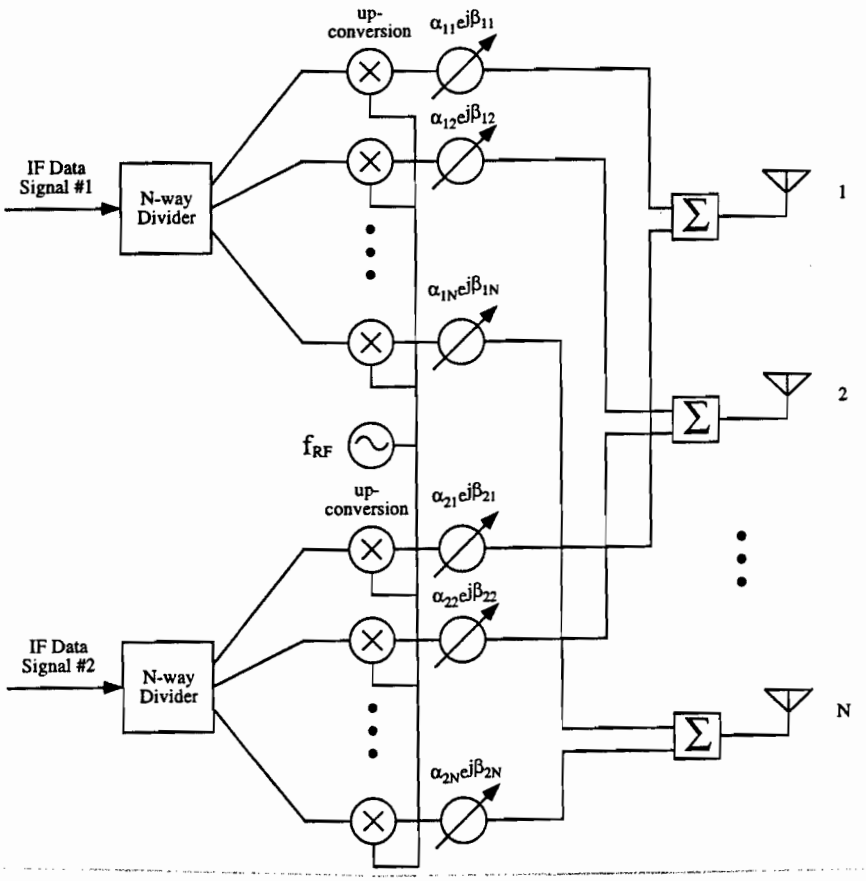

Figure 2.5 : Multiple beamforming by summing individual beams.

The current beamforming software used for RDRN was developed by S. Haas and D. Petr [4]. The algorithm takes the number of beams and the locations of users surrounding a transmitter and calculates the steering angles and relative beam power such that a local maximum in the minimum signal to interference ratio is achieved.

2.2.4 Beamforming for Arbitrary Modulation Schemes

Beamforming is only of use in a communication systems when its carrier frequency is modulated with some information bearing signal. Beamforming in this case can be described for a generic modulation scheme as follows[5]. Let the signal samples be represented by the vector

$$s = (s_{-\infty}, \cdots, s_{-1}, s_0, \cdots, s_t) \qquad (2\text{-}2)$$

where s is assumed to include the time index t implicitly. The most general form of modulation can be expressed as

$$x(t) = \mathrm{Re}[\alpha(s)\exp(j2\pi f_{IF}t + \phi_0 + \Phi(s))] \qquad (2\text{-}3)$$

where $\alpha(s)$ represents any form of amplitude modulation, f_{IF} is the IF carrier frequency, ϕ_0 is an initial phase, and $\Phi(s)$ represents any form of phase modulation. In most modulation

schemes, $\alpha(s)$ will reduce to $\alpha(s_t)$ where t represents the current time index or in phase shift keying, further reduces to a constant α. $\Phi(s)$ can represent Continuous Phase Frequency Shift Keying (CPFSK) schemes, of which Minimum Shift Keying (MSK) is a special case. It can also represent all Phase Shift Keying methods where the dependency reduces to $\Phi(s_t)$, or even coded modulation schemes like Trellis Coded Modulation.

Beamforming introduces an additional relative phase and amplitude of the signal going to each antenna element. Thus, the modulated signal of a single user $x_i(t)$ is modified to

$$x_{ij}(t) = \mathrm{Re}[A_{ij}(t)\exp(j\phi_{ij}(t))\alpha_i(s_i)\exp(j2\pi f_{IF}t + \Phi(s_i))] \qquad (2\text{-}4)$$

where subscript i refers to a user IF signal index and j refers to a specific element of a phased antenna array. Thus, the composite signal going to an element is given by

$$X_j(t) = \sum_i \mathrm{Re}[A_{ij}(t)\exp(j\phi_{ij}(t))\alpha_i(s_i)\exp(j2\pi f_{IF}t + \Phi(s_i))] \qquad (2\text{-}5)$$

Equation 2-5 is the per antenna element summing operation that appeared in Figure 2.4. Implementing phase shifts and amplitude control on RF signals can be done at frequencies up to 10 GHz. The devices used to do this are expensive and prone to elaborate calibration requirements in phased array systems as will be discussed in the prototype hardware implementation section of Chapter 3. Manipulation of the phase and amplitude at RF is however unnecessary. This is because relative phase shifts at the intermediate frequency are maintained after upconversion. This can be shown as follows. If an IF sinusoid $x(t)$ is upconverted to RF we have

$$x(t) = \cos[2\pi f_{IF}t + \phi_{IF}] \qquad (2\text{-}6)$$

and

$$X(t) = x(t)\cos[2\pi f_{RF}t] \qquad (2\text{-}7)$$

where f_{IF} is the IF frequency and f_{RF} is the RF carrier frequency. Expanding $X(t)$ results in

$$X(t) = \frac{1}{2}(\cos([2\pi(f_{RF} - f_{IF})t - \phi_{IF}] + \cos[2\pi(f_{RF} - f_{IF})t + \phi_{IF}]) \qquad (2\text{-}8)$$

then filtering and simplifying results in

$$X(t) = \cos[2\pi(f_{RF} + f_{IF})t - \phi_{IF}] \qquad (2\text{-}9)$$

where it is clear that the relative phase changes at IF are preserved after the upconversion. This makes the task of applying the complex weights needed for beamforming a much easier and less expensive task.

2.2.5 Hardware Methods for the Application of Complex Weights

Various analog and digital techniques for applying the needed complex weight exist. Digital Beamforming (DBF) techniques are the preferred method and of course require some type of digital control over the complex weights. Several analog techniques are briefly presented that make the digital design choices more clear in purpose.

2.2.5.1 Analog Control of Phase and Amplitude. The current predominant technology used to implement attenuators at RF frequencies up to several Giga Hertz are Gallium Arsenide (GaAs) Field Effect Transistors (FET). They are used as voltage variable attenuators where the controlling voltage is applied to the gate of the FET. They are widely available from many manufactures in inexpensive matched 50• surface mount packages. Unfortunately they impart a phase shift that is a non linear function of the level of attenuation. Analog phase shifters suffer similar problems and both require involved calibration schemes.

2.2.5.2 Digital Control of Phase and Amplitude. Digitally manipulating the phase of data at RF rates is computationally unfeasible and as previously mentioned unnecessary. Taking advantage of the fact that phase shifts and relative amplitudes are maintained after up conversion it is possible to cost effectively modify the lower frequency IF signals. Directly generating the IF signals with an arbitrary waveform generator is the most straight forward way to achieving application of the desired complex weights. The technique used for this function in the RDRN proof of concept system is summarized next and presented in detail in Chapter 3. A comprehensive and up to date overview of digital beamforming techniques and implementations can be found in [6].

2.2.5.3 Combined Modulation and Application of Complex Weights. Numerically Controlled Oscillators (NCOs) can use DSP techniques to digitally modulate an internally generated sinusoid with externally provided complex weights. Through proper application of the complex weights any M-PSK or M-QAM modulation techniques can be used. However, if modulation changes take place on a relatively slow basis or are fixed then simplifications are possible. If the steering angles and modulation schemes for the multiple beams change on the order of tenths of seconds, then the most rapidly changing component is the data symbols which for the presented prototype is 1 megasymbols per second per beam. Further simplifications arise if frequency modulation is not required and the modulation type is constrained to amplitude and phase modifications. These constraints allow a simple, cost effective, M-PSK and/or M-QAM modulator and simultaneous phase shifter design that is the main subject of this paper. This flexible beamforming software radio based IF modulator is now presented.

2.3 The Beamforming Transmitter Implementation

The goal of RDRN is to develop a proof of concept system. It must first and most simply show that its various elements can work together to achieve the desired goals. For instance the main goal of spatial frequency reuse by beamforming can be demonstrated by forming a minimum of two beams either on the transmit or receive data links. This however would only be

the minimum required. The minimum requirements were nearly always exceed with an attempt to best balance the given cost and time limitations.

The required specifications of the prototype are given next and then the most important self imposed constraints that affected the system design are discussed before the hardware system is presented in detail.

2.3.1 Prototype Implementation Specifications

The RDRN prototype system is required to demonstrate spatial frequency reuse by supporting at least two separate mobile users from the same antenna at the same frequency. A high speed data channel of at least 1 Mbps should simultaneously be available in any of the directional beams formed. Multiple mobile users that are physically located within the same directional beam should be handled by a Time Division Multiple Access (TDMA) scheme. The specifications chosen for the proof of concept system are summarized in Table I.

Table I Prototype Design Specifications	
Maximum number of simultaneous beams per edge switch or mobile node	4
Maximum transmit rate (only 1 beam active)	8 Mbps
Maximum receive rate	2 Mbps
Minimum number of Tx/Rx frequencies	4 (2 pairs)
Maximum Transmit Distance at a Bit Error Rate (BER) of 10-5	10 km
Modulation types	Any AM, PM, or QAM (No FM)

2.3.1.1 Radio Frequency Requirements. The relatively high data rates required necessitates a large section of contiguous and available bandwidth of at least 20 MHz. The first publicly available sections of the RF spectrum with this capacity are the Industrial Scientific and Medical (ISM) bands at 915 MHz and 2400 MHz. These bands however are crowded by as the name implies industrial equipment that it is unlawful to interfere with. Equipment in these bands typically transmits with less than 1 Watt of power. The need for RDRN to transmit up to 10 km requires high power levels that would defiantly cause interference to these bands.

The Amateur Radio Service (ARS) band located at 1.27 GHz was chosen instead. It has a contiguous 60 MHz of bandwidth from 1240 to 1300 MHz and a transmit power limit of over 2000 Watts Peak Envelope Power (PEP). The only requirement is that anyone transmitting in the bands be a FCC licensed amateur radio operator and participants in the RDRN prototype have met this requirement.

2.3.1.2 Intermediate Frequency Requirements. Regardless of whether beamforming is done by analog or digital means or if it is done at all some type of IF information bearing signal must be upconverted. The process of upconversion as will be detailed later produces sum and difference frequencies in addition to other non linear products. Only the signal of interest, usually the sum, can be passed on, amplified and put out over the antenna in order to avoid

interfering with neighboring frequency channels. Extracting the signal of interest is done with what is called an image-reject filter.

In order for the image-reject filter to be physically and cost effectively feasible the IF frequency must be sufficiently high enough so as to place the difference frequency ($f_{IF} - f_{LO}$) far enough away from the sum frequency ($f_{IF} + f_{LO}$) so that it can be filtered out. The higher the RF frequency the higher the IF frequency required. Operation of the RDRN system in the ARS band at 1.27 GHz places the practical minimum IF frequency at 70 MHz with 150 MHz being more the ideal. Digital beamforming places competing requirements on the IF signal frequency however. The digital clock limits on D/A converters constrain how high the IF frequency can be. The IF frequency chosen for the RDRN prototype was 70 MHz.

2.3.2 Prototype Implementation Constraints

Due mainly to complexity driven cost constraints the prototype hardware built for RDRN was limited to form a maximum of four directional beams and only in the transmit direction of the full duplex links. The antenna system design was governed by similar constraints due the fact that the number of active antenna elements and the associated driving hardware is the major controlling factor in the cost a phased array system. Therefore the multi element phased array used for the transmit link was limited to eight elements.

Several additional limitations are key to the design of the presented system. The details as to why these constraints save money, time and complexity will be shown in the remaining sections. First, no frequency modulation is used so that all data streams modulate the same frequency IF carrier. This constraint means that regardless of the number of beams, end users, or the complexity of the modulation being used, only the amplitude and phase of the composite IF signal can be changed (i.e. the system is linear). Second, the modulation schemes and steering angles must change at a rate several orders of magnitude slower than the symbol rate. Finally, the symbol rate must be constant and synchronous across all of the beams being formed.

Restricting the RDRN system to the above constraints makes possible a hardware implementation that combines the task of beamforming and flexible IF modulation into a single cost effective solution. This flexible beamforming software radio based IF modulator in now presented in detail.

2.3.3 A Flexible Beamforming Software Based IF Modulator

Figure 2.6 shows an IF waveform synthesizer that has already been developed as a working prototype that provides the capability to generate a 70 MHz IF waveform with precise control over its phase and amplitude.

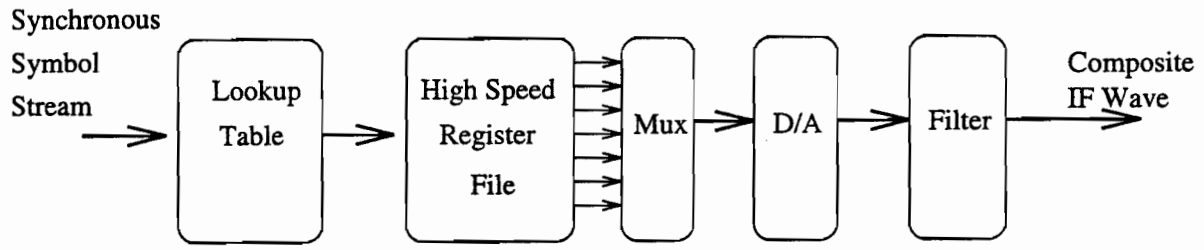

Figure 2.6: Semi-arbitrary IF modulator and beamforming architecture.

The IF waveform is controlled by a lookup table that contains a representation of the desired waveform for a specific combination of 8 bits of a lookup vector. These 8 bits can represent any valid combination of users, beams, and data for the currently defined modulation schemes under use. The lookup table then contains the proper samples required for the D/A converter to generate one full 360• cycle of a sinusoidal waveform of the desired amplitude and phase. These samples are loaded into a high speed register file at every symbol change. The lookup tables and waveform generators are independent for each antenna element. This allows beamforming by varying the relative phase and amplitude for a given lookup vector across the eight lookup tables, one for each antenna element.

2.3.4 Lookup Table Generation

Determining how a particular edge switch or remote node will form its beams is the first step in building the lookup tables. It is the function of the previously mentioned beamforming software by S. Haas and D. Petr to calculate a solution to optimize this process. Once the steering angles and relative powers are known, the hardware must be able to deliver the energy to the proper location and with the correct information. If all the information necessary for modulation, calibration, and beam steering is known, the lookup tables can be calculated.

The required phase shift and amplitude for each element is known for a particular beam as characterized by the beamforming algorithms used. The IF waveform that represents each symbol for that beam is calculated. For a given combination of all symbols across each desired beam the calculated IF waveforms are then summed to form a composite waveform for every symbol combination and antenna element. This composite waveform is processed through a set of calibration, normalization, and quantization routines to produce a set of samples, unique for each symbol combination and element. These stored samples are the numbers that when repetitiously passed directly to the D/A converter will produce an IF sinusoid waveform with the currently desired phase and amplitude. The lookup tables are then filled with every combination of these composite waveforms, for the specific beam scenario chosen. Each time a steering angle or modulation change is desired the tables must be recalculated and downloaded again.

Storing the samples required to generate all possible combinations of IF waveforms can quickly consume large quantities of memory if the number of data input bits controlling the lookup is not kept small. The size of the needed memory grows as a exponential function of sum of the number of required beams and the number data bits. The number of beams for the RDRN prototype was therefore limited to four and the maximum number of data input bits was limited

to eight. The data bits can be partitioned and repartitioned into multiple beams each with its own modulation type. The frames within a beam can be multiplexed using a TDMA scheme to as many as 64 users. The sum of the bits needed per symbol interval, independent of the number of simultaneous beams, must not exceed the limit of eight. The symbol interval for the prototype system is 1 μs as will be detailed the next section. As an example, consider 4 simultaneous beams, with three different modulation schemes as shown in Table II.

Table II Example Lookup Table Distribution

Beam	Modulation	Bits/Symbol	Data Rate
# 1	BPSK	1	1 Mbps
# 2	QPSK	2	2 Mbps
# 3	8-PSK	3	3 Mbps
# 4	QPSK	2	2 Mbps
Totals		**8 bits**	**8 Mbps**

A dynamically reconfigurable software radio is made possible by using a software process that calculates the tables for a desired choice of number of beams, their respective steering angles, and their modulation types.

2.3.5 IF Output

The purpose and function of the semi-arbitrary waveform generator designed for use in this project can be better understood by examining the physical structure and timing of the desired IF waveform. Eight samples are used per 360• cycle of the IF waveform to provide a good spurious free dynamic range. To generate the desired 70 MHz IF directly would require a D/A converter running at 560 MHz. Another approach would be to generate a lower frequency first IF and upconvert to a second IF, filter, and then upconvert again to the desired RF frequency. An alternative method takes advantage of the first image frequency that appears after digital to analog reconstruction. By proper choice of the sampling frequency, F_S, and the fundamental frequency, F_C, the first image can be placed at the desired IF, bandpass filtered and then upconverted directly to RF. In order to repetitiously use the same samples over an entire symbol interval, the desired fundamental frequency, F_C, must be chosen so that the samples used to represent it repeat as an integer sub-multiple of F_S. In the system being presented, F_S was chosen to be 80 MHz and F_C to be 10 MHz. The IF waveform repeats every eight samples and the first frequency image appears at F_S-F_C (80MHz - 10 MHz = 70 MHz). The image at 70 MHz must be filtered out by a narrow bandwidth bandpass filter. The quality of the alias is limited by the bandpass filter and the D/A's number of bits and rise time characteristics. Figure 2.7 shows the relative magnitude of the first and second alias with respect to the fundamental as measured from the prototype's D/A converter.

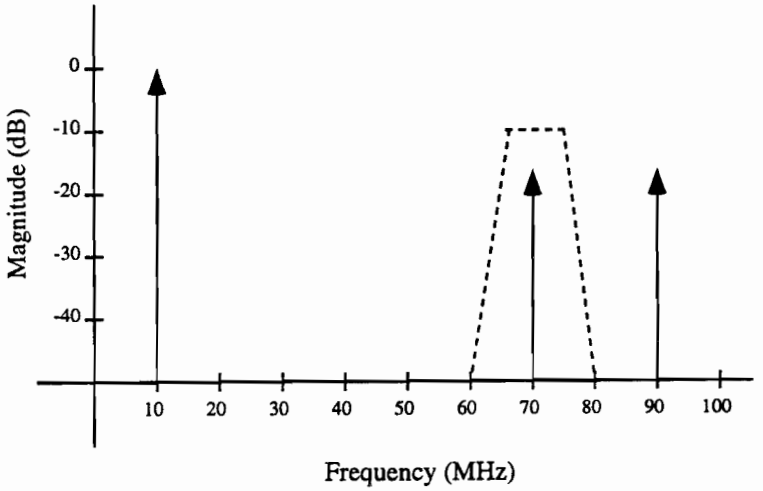

Figure 2.7: 10 MHz IF waveform and its first two reconstruction images.

Even though there is a 16dB loss, the signal-to-distortion ratio can be kept as high as required by picking a converter with the necessary number of bits. Most importantly, changes in both the amplitude and phase of the 10 MHz signal are linearly translated into all of the image frequencies produced. This unconventional procedure eliminates the need for an upconversion to a second IF frequency.

2.3.5.1 IF Output timing relationships. The OEM receivers chosen for the first stage of the prototype system limit the maximum symbol rate to 1 Msps. In particular, two separate receivers are available at 1 Mbps (BPSK) and 2 Mbps (QPSK) The symbol rate of a 2 Mbps data stream using QPSK without any type of fractional rate encoding is simply 1 mega symbols per second (Msps). Figure 2.8 shows the timing of the 10 MHz IF waveform where the symbol rate of 1 Msps is filled with 10 identical series of 8 samples each.

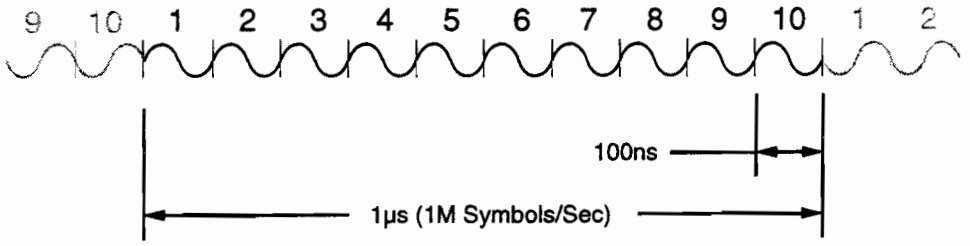

Figure 2.8: Output timing relationships of the 10 MHz IF output.

This process repeats once every micro-second with the output samples changing to represent the appropriate phase shift and amplitude of the desired IF signal. In the prototype each of the eight samples that are held in the register file are repetitiously cycled through ten times as seen in Figure 2.8. This system design, in addition to the frequency modulation constraint, is not capable of any type of pulse shaping of the output waveform. Finally, the symbol changes among all simultaneous beams are constrained to be synchronous.

2.3.6 The D/A Converter

The D/A converter being used to produce the 10 MHz IF output is the Harris Semiconductor HI5731. It is a 12 bit, 100 MSPS high-speed D/A Converter. It generates a current output, as do most high speed D/A converters, and it must ideally see a real 50• load to ensure proper settling. This fixed termination develops an output voltage ranging from 0V, for full scale minus, to -1V for full scale plus. One of the enumerated 10 MHz IF cycles depicted in Figure 2.8 is shown in detail in Figure 2.9 as it appears at the terminated output of the D/A.

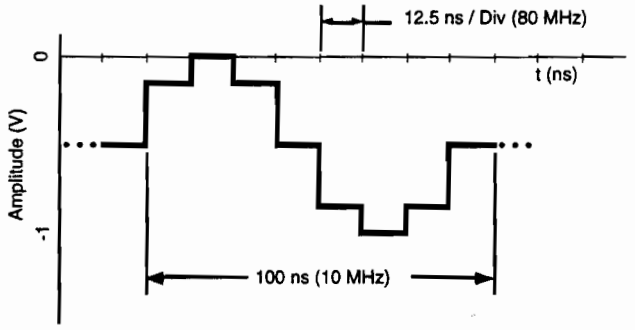

Figure 2.9: One Section of the 10 MHz IF Output from the D/A Converter.

2.3.6.1 I/V Conversion of the D/A Output. The required 50• termination load for the D/A converter is incorporated into a DC coupled high-speed current-to-voltage conversion stage that is implemented with a Harris HFA1112 buffer Op-Amp. This implementation was taken directly from the HI5731 data sheet and is depicted in Figure 2.10.

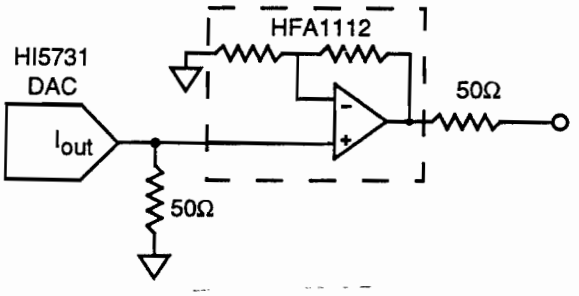

Figure 2.10: Current to Voltage Buffer Section.

All of the previously discussed modulation and beamforming hardware is contained on a single VME form factor card, one for each antenna element. This was done to keep the system modular and facilitate debugging, repair, and identical parts in case of a failure. The buffered 10 MHz IF output signal is then passed via a SMA cable onto the RF upconversion stage that is separate from the VME chassis holding the transmit cards.

2.3.7 IF to RF Up-Conversion

The buffered 10 MHz IF input from the previous stage is now filtered with a 70 MHz bandpass filter. This bandpass filtering is not implemented directly on the VME card so that any spurious out-of-band noise picked up on the SMA feed cable is rejected. The filter is AC coupled and the resultant output is free of any DC component without the need for any troublesome bipolar offset adjustment circuitry. The IF signal is now a 70 MHz IF whose relative amplitude and phase with respect to the synchronized and identical D/A converters used for the other seven IF outputs is under precise control.

The IF outputs from each of the eight beamform cards must be upconverted in tandem in such a way that the relative amplitudes and phase shifts between each of them are maintained all the way up to the antenna. Figure 2.11 shows, at the block diagram level, the system that is being used to implement this tandem or "coherent" up conversion.

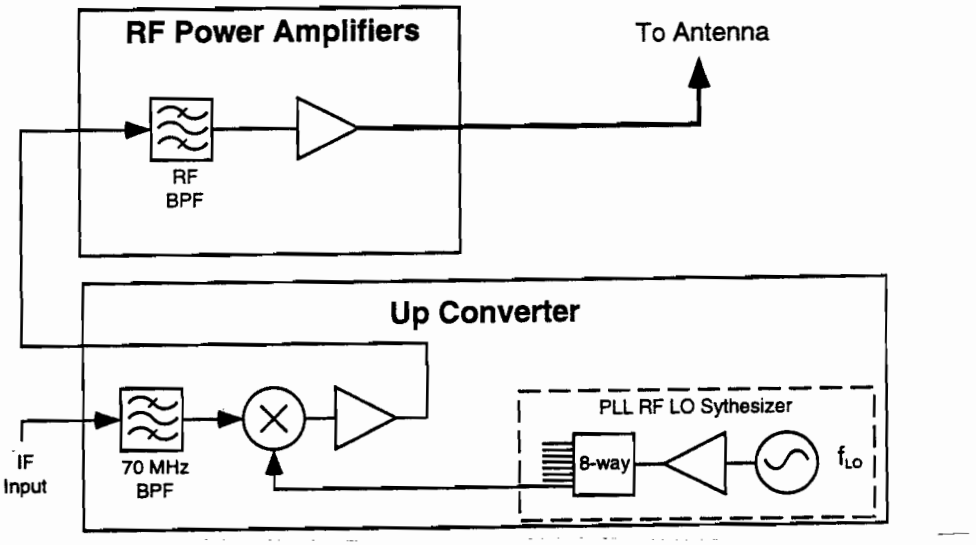

Figure 2.11: RF Upconversion block diagram.

The 70 MHz signal is then buffered and directly input into a double balanced mixer that is driven by one of the eight local oscillators.

2.3.7.1 RF Local Oscillator. Key to the proper operation of this system is that each of the eight separate RF mixers gets a local oscillator signal with the same phase. This is achieved by use of a passive 8-way power divider to distribute the same RF local oscillator to each mixer. The RF LO is a synthesized phase-locked oscillator capable of a 900-1600 MHz operating range. The LO has a parallel interface allowing its operating frequency to be changed under software control as shown in Figure 2.12.

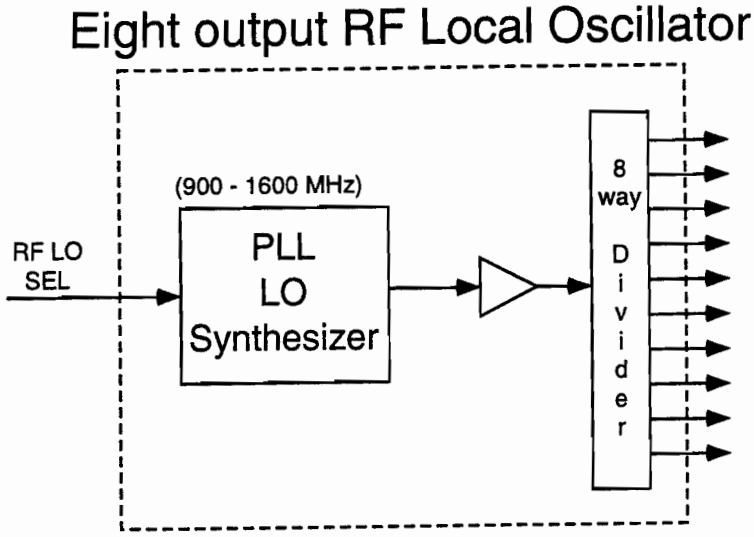

Figure 2.12 : Frequency Selectable RF Local Oscillator.

The initial prototype works in an ARS frequency band from 1240-1300 MHz. , However, the entire system is designed to be capable of operation at up to 2500 MHz with only a few modular RF part changes, namely the RF LO and a single bandpass filter. The next stage is the RF power amplifier subsystem.

2.3.7.2 RF Power Amplifiers. The input signal to this stage is the output of the RF mixer. This signal is comprised mainly of the sum and difference frequencies produced by the mixer. It also contains LO feed through, in addition to other non-linear products and sums. The signal of interest is the sum frequency that falls in the transmission band from 1240-1300 MHz. This signal is filtered out from the others by an image reject bandpass filter, pre-amplified and fed to the RF power amp. The RF power amp is a 1.5W, 1240 to 1300 MHz, Mitsubishi M67715 linear amplifier. The proper operation of the beamforming algorithm requires all chains of amplification to be linear. Therefore the maximum output of the amplifier is limited to 680 mW to avoid compression on the output signal.

2.3.7.3 Calibration. Before the amplified signals reach the antenna they are passed through two back-to-back 3-port directional couplers that form a dual directional coupler. This series of couplers is used to sample the amplitude, phase, and reflected power of the signals to calibrate the system. The system can now automatically perform self-calibration routines by sending out from each of its eight transmit cards identical sinusoids in both phase and amplitude. Due to discrepancies in local oscillators, IF and RF amplifiers, mixers, cables, etc., the signals reaching the antenna have some phase and amplitude discrepancies. The sampled information for this error can then be used to generate calibration tables that are used by the software. The signal is finally fed to its respective element of the multi-element transmit array. This calibration system has yet to be designed.

2.3.7.4 Antenna Array. The transmit section uses a linear equally spaced eight element phased array optimized to work at the center of the 23 cm (1240-1300 MHz) amateur band. The array consists of eight, quarter wavelength monopoles, equally spaced at half wavelengths of the 23 cm operating frequency. A digital compass is mounted on axis with the array to provide the physical orientation of the antenna. The antennas back ground plane prevents the antenna from radiating

in the backwards direction. The field of converge is limited to 180• in the proof of concept system. Work is currently underway to investigate conformal antenna arrays and their use in generating multiple steered beams with 360• coverage [7].

2.3.7.5 10 MHz IF to Antenna Block Diagram. The complete chain from the 10 MHz IF output of the IF card all the way to the transmit antenna is available as a block diagram in Appendix A. It contains detailed information such as the manufacture's and part numbers of all devices used in the RF section of the hardware. It additionally contains a RF power "link budget" for all the parts.

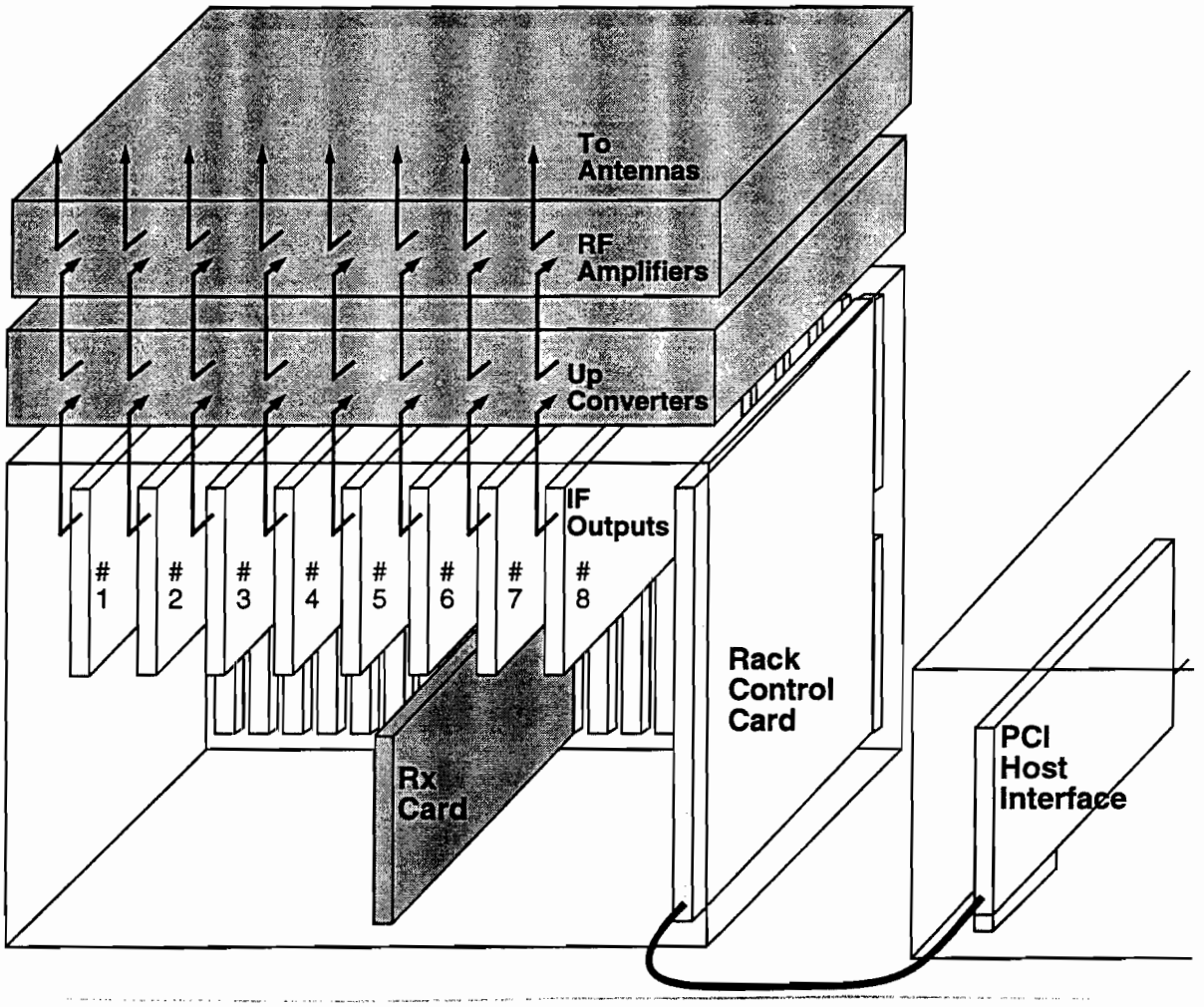

Figure 2.13: Component level view of the hardware.

2.3.8 Physical Construction Overview

The entire prototype system discussed is contained within a mobile 19" rack mount case. The case has removable front and back covers so that the system can be stored and taken to testing and demonstration sites. Figure 2.13 shows a component level view of the physical setup of a remote node. All eight of the transmit cards are contained in a VME chassis along with a card to control them and talk to the host PC. An edge switch has the same hardware components except that it will have an OC-3 fiber ATM card and typically have additional receivers. The host is a Penitium®-based PC running a UNIX derivative.

The position of the components as they are housed in the mobile rack mount case is depicted in Figure 2.14.

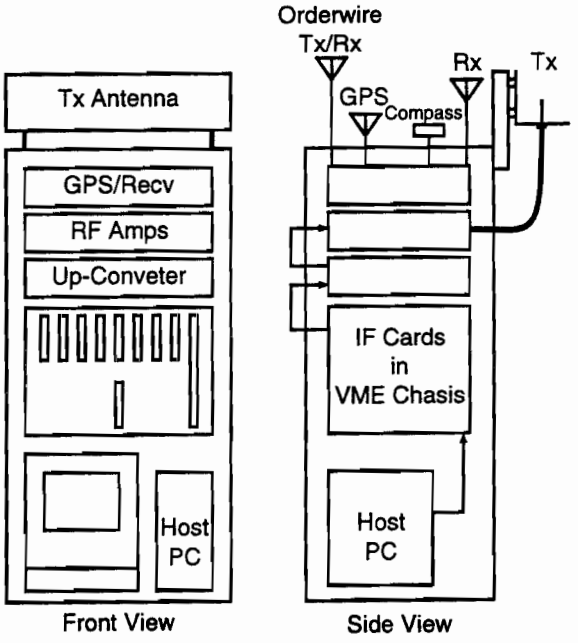

Figure 2.14 : The Antenna and Rack Mount Case.

2.4 Design of A Digital Beamforming Receiver

There is potential commercial value in the practical application of adaptive antenna technology. An adaptive array at the transmitter is capable of steering a radiation pattern maxima toward a desired mobile, which can increase system capacity. In addition, by using an antenna array at the receiver to spatially separate and reject multipath energy, higher bit rate services can be provided.

Despite the advantages adaptive array antennas offer, their application in commercial mobile communication systems is not common. This is partly due to implementation complexities. Our task here is simply to implement a digital beamforming receiver using commercially available signal processing devices.

2.4.1 Receiver Beamforming

The beamforming network of an adaptive antenna array can be implemented using either analog technology at Radio Frequency (RF) or Intermediate Frequency (IF) or digital circuit technology at baseband. RF and IF techniques, although once popular, are relatively inflexible. The digital approach offers the highest precision, flexibility and capacity for future development.

In traditional analog beamforming the RF signal at each antenna element is down converted to IF and the phase is changed by using analog phase shifters. At this point, all the phase shifted signals are summed. The beamformed signal is then down converted to baseband and successfully converted to a digital signal.

As a practical matter only a limited number of beams (less than 10, in general) can be formed at the RF or IF stage with passive phased-array antennas using analog technology. The disadvantages of this technique are related to difficult control of the side lobe level, high loss, absence of individual beam shape control, complex construction and corresponding heavy equipment.

Unlike analog beamforming, digital beamforming receivers digitize the received signals at the element level, then processes these signals in a special-purpose digital processor to form the desired beam(s).

2.4.2 DBF Receiver Design

The Digital Beamforming (DBF) Receiver implemented here performs two functions: Beamforming and QPSK Demodulation. The block diagram of the digital beamforming receiver is shown in Figure 2.15.

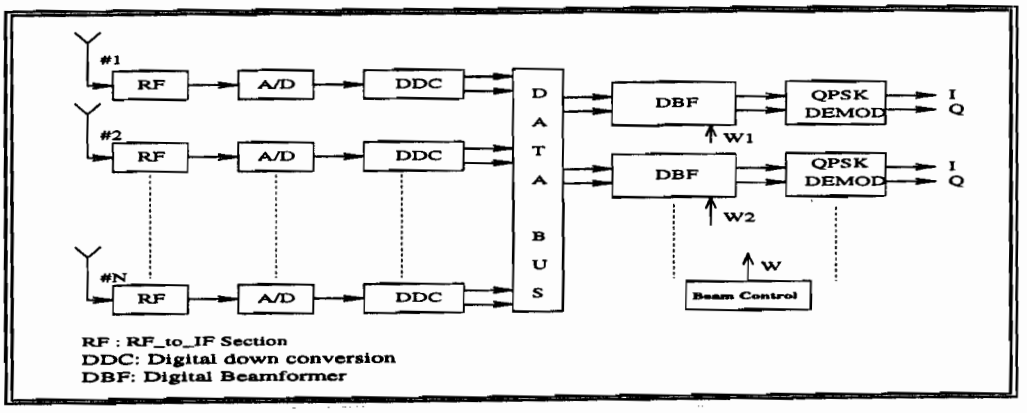

Figure 2.15: Block Diagram of the Digital Beamforming Receiver

The received signal is digitized at the IF with one receiver section for each antenna element. After the input signals are digitally down converted to baseband, they are processed in a digital beamformer and the signal is demodulated. The RF section is a conventional superheterodyne receiver, which establishes the overall receiver sensitivity, downconverts the signal to the intermediate frequency, and provides selectivity in the bandwidth of interest.

The IF signal is centered at 70 MHz with a bandwidth of 5 MHz (data rate of 10 Mbps with QPSK modulation). Hence, to digitize this IF bandpass signal, we use bandpass sampling, which consists of sampling the signal at a multiple of the information bandwidth, but at a rate which is much lower than the Nyquist frequency.

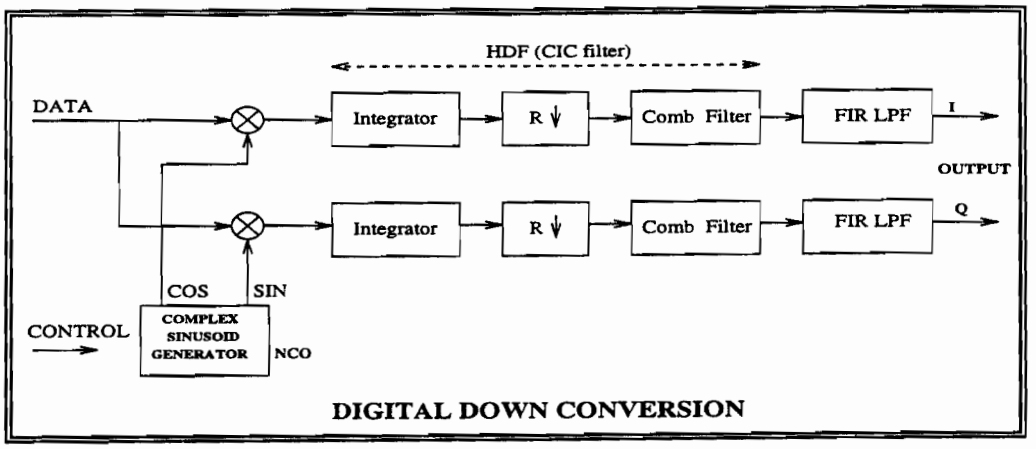

Figure 2.16: Digital Down Conversion Block Diagram

In digitizing the analog received signal, one A/D converter is required for each antenna element. The final step in the demodulation process is to translate the sampled IF signal into a complex baseband signal. The complex baseband signal retains the magnitude and phase detail of the original real input signal. Low-pass filtering and decimation of this signal to a lower sample rate will reduce the number of samples needing to be processed The Digital Down Conversion (DDC) process is illustrated in Figure 2.16.

Filtering the input signal reduces its bandwidth resulting in a highly oversampled signal. A reduction in sample rate eliminates redundant samples and speeds computation, and also has a noise reducing and an anti-aliasing effect. Filter requirements of linear phase and high decimation rates beyond 16000 make standard FIR filters with orders greater than 100,000 impractical, as they require many time consuming multiply and accumulate (MAC) operations.

The DDC section circumvents this problem in both I and Q data branch by using a 2-stage filter architecture. It uses a high-decimation filter (HDF) for low pass filtering followed by a standard FIR (finite-impulse response) compensation filter for final wave shaping. The HDF is comprised of a 5-stage integrator, decimation register and a 5-stage comb filter. This kind of filters is called a CIC (cascade-integrate-comb) filter and it results in a more economical hardware implementation. The economy of CIC filters derive from the fact that no multipliers are required; no storage is required for filter coefficients; intermediate storage is reduced by integrating at the high sampling rate and comb filtering at the low sampling rate, compared to the equivalent implementation using cascaded uniform FIR filters.

The digital beamformer, a very fast digital processor, forms multiple beams by finding the product of the set of received samples from the array of antenna elements and the sets of weights that shape the beams originating from the antenna. The complex weights are determined from the

beam orientation. The core of the beamforming operation is performing the complex multiplication and accumulation of the complex weights and the received samples.

A feasible solution has been found to be the use of high-speed ASSPs (Application Specific Signal Processing circuits) that perform a CMAC (Complex Multiply and Accumulate) operation within one clock cycle. Since we need 8 CMAC operations in 1 symbol duration, the ASSP has to operate at a minimum of 40 MHz. ASSPs are available that operate above 50 MHz and hence this seems to be an achievable approach for the design. To form any number of beams, we require the same number of CMAC ASSP chips.

The final stage of the receiver is a standard QPSK demodulator. Its input is the I and Q output from the beamformer. The Harris device, HSP50210 (Digital Costas Loop) performs many of the baseband processing tasks required for the demodulation of BPSK, QPSK and OQPSK waveforms. These tasks include matched filtering, carrier tracking, symbol synchronization, and AGC. This QPSK demodulator takes the I and Q symbols from the beamformer and detects the beam to generate the data. We have to use one QPSK demodulator for each beam we want to receive.

2.4.3 Implementation

We validated the functionality of the design by implementing and testing each individual section of the beamforming receiver. The A/D converter is the 10-bit Harris HI5703 which is used to digitize the incoming 70 MHz IF signal. The converter is capable of operating up to 40 MHz. The receiver is designed using HARRIS chips HSP50110 (DQT) and HSP50210 (DCL). Due to the use of these devices, the digital radio is easily reconfigurable via software. The reconfigurable digital radio design is shown in Figure 2.17.

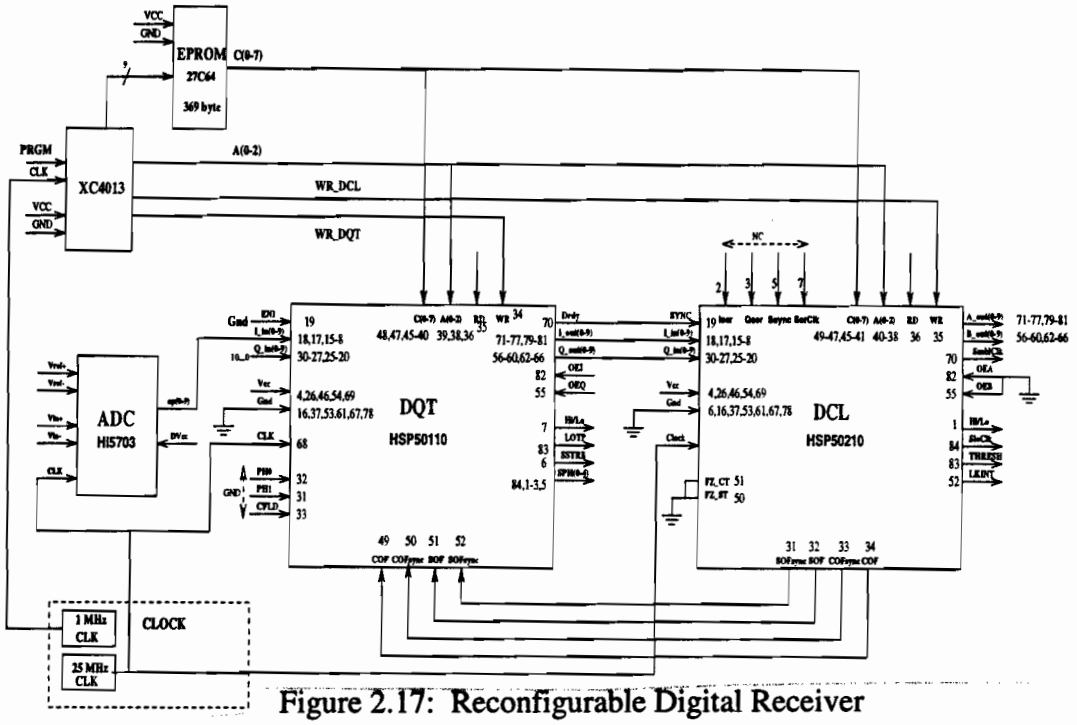

Figure 2.17: Reconfigurable Digital Receiver

The HSP50110 and HSP50220 chips are to be programmed for the particular specifications of the receiver by loading the registers in these chips via the microprocessor interface. The main programmable parameters of the receiver are:

• Local Oscillator (HSP50110): The center frequency and the phase offset of the local carrier can be programmed. The carrier frequency can be adjusted dynamically to account for the carrier phase offset effects.

• Input Level Detector Threshold (HSP50110): This is used for IF AGC control. The level detector output is to be externally averaged to set the gain of an amplifier in front of the A/D which closes the AGC loop.

• Baseband AGC (HSP50110): The level of the Mixer output is gain adjusted by baseband AGC around the Low pass Filtering. This baseband AGC provides the coarse gain correction necessary to help maintain the output of the HSP50110 at a signal level which maintains an acceptable dynamic range.

• Low Pass Filter configuration (HSP50110): The low pass filter can be configured as a 1-stage or 3-stage CIC filter.

• Re-Sampler config. (HSP50110): The re-sampler sets the output sample rate by controlling the sample rate of the decimation filters. The output sample rate can be adjusted dynamically to synchronize with baseband waveforms.

• Matched Filtering (HSP50210): We can use Raised Root Cosine (RRC) or Integrate \& Dump (I/D) filter for matched filtering. The number of samples to be integrated per symbol can also be programmed.

• Baseband AGC (HSP50210): This is used to maximize the dynamic range, adjust for signal to noise variations and maintain an optimal signal level at the input to the soft decision slicer.

Figure 2.18 shows the eight receiver sections comprised of an RF section, HI5703 (ADC) and HSP50110 (DQT).

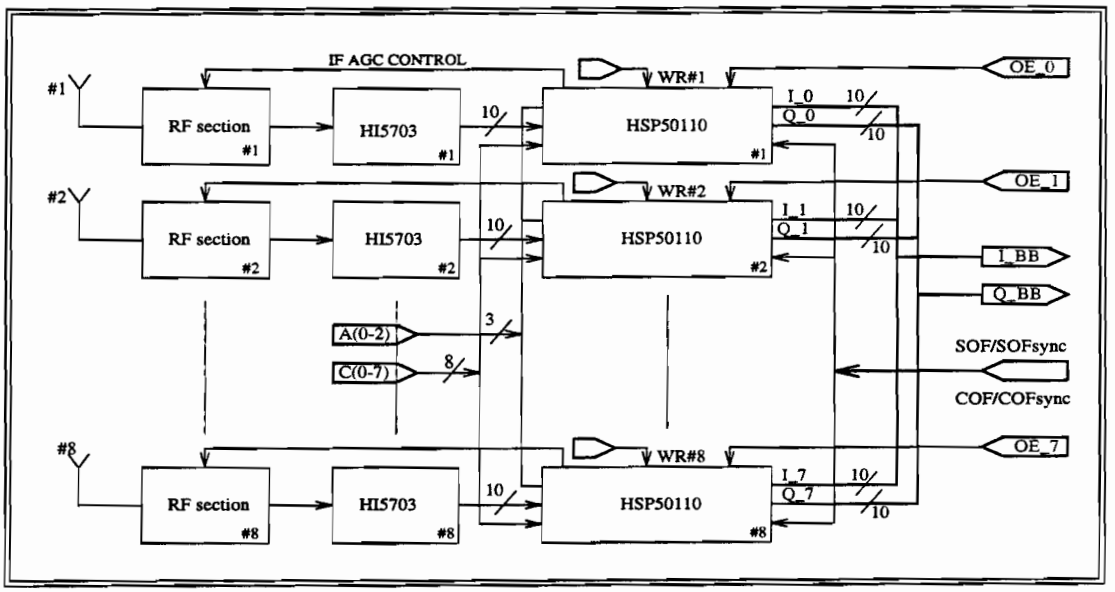

Figure 2.18: DBF Receiver Front-End

Each receiver section consists of an RF section which down converts the RF signal to IF signal. The HI5703 digitizes the IF signal at 25 MHz. The digitized samples are given to HSP50110 operating at 25 MHz. The output of HSP50110 is the I and Q baseband samples of the received signal. All these signals are tied together to form a bus and the output is given to the next section. The OUTPUT ENABLE (OE) signal which is provided from the next section selects the output from a single HSP50110, tri-stating all the other outputs. The HSP50110s are programmed using the programming section shown in Figure 2.19.

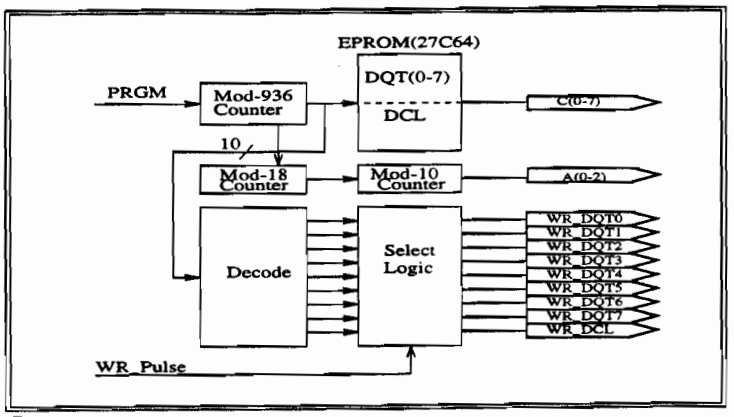

Figure 2.19: Programming Logic Design For DBF Receiver

Figure 2.20 shows the beamforming and demodulator section. The dotted portion of the Figure is designed to reside in a Xilinx FPGA XC3195A. It provides the OUTPUT ENABLE (OE) signals to HSP50110s. The HSP45116A chip operating at 40 MHz implements the complex multiplication and accumulation of this data with the complex weights stored in sequential logic. The PAL logic which controls the 10-bit multiplexer operates at 80 Mhz.

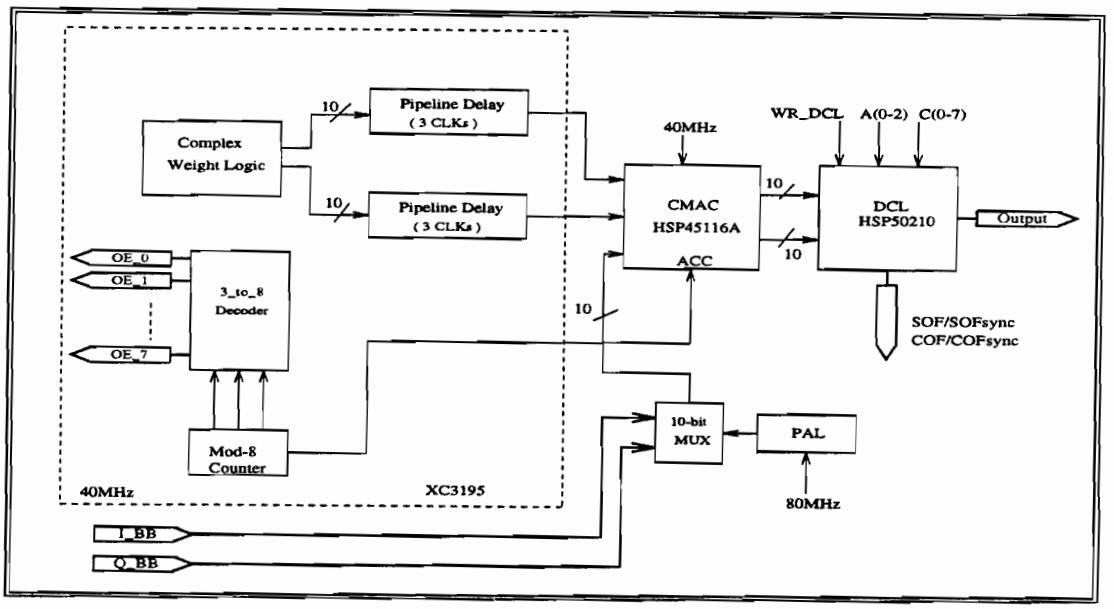

Figure 2.20: DBF Receiver Beamforming Processor

In the beamforming section, the complex weights are to be stored in memory. We need a memory of eight 10-bit complex words. The memory needs to be accessed at 40 MHz. For this application, a logic circuit is implemented in the XC3195A to store the components. A mod-8 counter is designed to represent the 8 different complex words.

The beamforming logic resides in one XC3195 FPGA. It performs the decoding and pipeline delay functions necessary to do prior to beamforming. For more beams, the same FPGA can be used. To form more than one beam, we just need to add more CMAC and HSP50210 chips in parallel. The logic to incorporate more number of beams can be implemented in this FPGA. Also, when we increase the number of elements, the logic can be changed in this FPGA along with the addition of the receiver sections, avoiding the change of physical hardware.

2.5 Summary

The radio transmitter/receiver system that was developed for the RDRN project represents a first step in the development and implementation of an end-to-end software radio system which incorporates beamforming at the transmitter. The next step will be to include beamforming at the receiver as well. In this project, transmitter beamforming helped us prove the concept of frequency reuse while giving us experience in prototype fabrication with RF hardware.

The radio receiver system used the latest techniques in digital signal processing, including undersampling at the Intermediate Frequency followed by inphase and quadrature downconversion to baseband via a numerical controlled oscillator (NCO). All demoduation and tracking algorithms were implemented digitally using application specific integrated ciruits.

The use of GPS as an integral part of the network was an invaluable innovation in that it simplified the transmitter beamsteering algorithm and allowed a simple table lookup procedure to be used. There is no doubt that this procedure will be eventually incorporated into radio systems

of this type because it relieves the radio processor from the requirement to adaptively configure the antenna pattern. While this project used an antenna array of limited size, future implementations will no doubt extend the size of the array to 32 or more elements to allow full 360 degree coverage.

The system performed quite well in field tests over a distance 10 Kilometers. The error rate was consistently within the link quality requirement. During the next phase of this system we will explore techniques for adapting the link to maintain consistently high throughput through the use of algorithms in the radio processor which adjust power level, coding depth, antenna pointing, modulation type and data rate.

2.6 Bibliography

[1] B. Ewy and C. Sparks "Rapidly Deployable Radio Network Proof of Concept System," TISL Technical Report TISL-10920- , University of Kansas, March. 1996

[2] J. Mitola. "The Software Radio Architecture," *IEEE Communications Magazine*, Vol. 33, No. 5, pp 26-38, May 1995.

[3] W. Stutzman and G. Thiele, *Antenna Theory and Design*, John Wiley & Sons, New York, 1981.

[4] S. Haas and D. Petr. "Beam Matlab Code." TISL Technical Report TISL-10920-03, University of Kansas, Jan. 1995

[5] B. Ewy and C. Sparks "A Flexible Beamforming Digitally Synthesized IF Modulator," ISCAS '96 Paper Proposal, TISL Technical Report TISL-10920-15, University of Kansas, Sept. 1995

[6] H. Steyskal. "Digital Beamforming at Rome Laboratory," Microwave Journal, Vol. 39, No. 2, pp 100-126, Feb. 1996.

[7] D. Chaterjee and R. Plumb. "Numerical modeling of antenna arrays for RDRN," TISL Technical Report TISL-10920-14, University of Kansas, Jan. 1996

[8] C. Anderson and J. Fakatselis, "Digital IF Sub-Sampling using the HI5702, HSP45116 and HSP43220," Technical Report AN9509.1, Harris DSP and Data Acquisition, April 1995.

[9] A. Ferina, *Digital Beamforming Antennas*, Prentice Hall, New Jersey, 2nd edition, 1993.

[10] B. Ewy, C Sparks, K. Shanmugan, J Evans, G. Prescott, "An Overview of the Rapidly Deployable Radio Network Proof of Concept System," Technical Report 10920-16, Telecommunication and Information Sciences Lab, July 1995.

3. ARRAY ANTENNAS FOR RDRN – DESIGN, ANALYSIS AND MEASUREMENTS

3.1 Introduction

This section provides a description of the work related to the development of the linear [1] and conformal cylindrical [2] arrays for use as transmit antennas in Rapidly Deployable Radio Networks (RDRN). The main purpose of this report is to illustrate the major milestones achieved Phase I and to identify the work that needs to be done for the future.

The design and implementation of the complete transmitter system for Phase I prototype included application of the Digital Beamforming (DBF) concept [3]. The DBF was employed to achieve spatial frequency reuse. The primary objective of Phase I was to demonstrate the beamsteering concept and to propose an antenna architecture for the next generation of transmitter designs. To that end, a cylindrical conformal microstrip antenna architecture and a new technique for realizing beamsteering and improved pattern control have been reported in [2]. By virture of its geometry a cylindrical array can provide 360° coverage in the azimuth. However the basic techniques of beamforming and beamsteering and their hardware implementation need to be understood. Thus it was necessary to acquire this experience by using an eight-element linear array. This simplified the design while at the same time provided useful insight in implementing the DBF technique.

Microstrip antennas are currently emerging as the state-of-art choice for microcellular wireless applications [4]. Various other element configurations [5-7], can be used in their place. However, microstrip antennas are lightweight, low-profile and easy to fabricate. These properties suggest their application to rapidly deployable radio networks is more appropriate than other types of elements.

Antenna arrays in cellular CDMA enhance channel capacity and provide spatial diversity [8-10]. In most cases these arrays are "smart" (or adaptive). Adaptive antenna arrays use algorithms which basically compute the complex excitation weights behind every element in a manner that the reuslting array pattern is suitable for the change in environment conditions. Some typical algorithms have been described in [11]. The extension of the adaptive algorithms to include mutual coupling effects in arrays appears possible by using the techniques suggested in [12, 13].

In this section the modeling of antenna patterns is discussed based on the methods presented in [14, 15]. These methods rely on the diffraction theory which is becoming an important tool in modeling r.f. propagation in a microcellular environment [16-18].

In the following section, relationship between DBF and conventional array theory is explained. The method by which linear array antenna patterns were modeled is described next. Comparisons with measured data are also included. This is followed by a brief description of the investigation into modeling of conformal cylindrical arrays. It is to be emphasized that similar

efforts have been reported in [19]. The investigations reported here have been presented earlier in [20-22].

It should be noted that only sufficient details are included so as to make this section self-contained. Detials for cylindrical arrays are included in [2].

3.2 Review of Array Theory and the Digital Beamforming Concept

The radiation pattern of an N-element array can be written [4, ch. 3] as

$$\vec{\mathrm{E}}(\theta,\phi)=\sum_{n=1}^{N} w_n \vec{\mathrm{g}}_n(\theta,\phi) e^{jk_0 \hat{\mathrm{u}}_R \cdot \vec{\mathrm{r}}_n}, \tag{3.1}$$

where

(i) $\vec{E}(\theta,\phi)$ is the total radiated field at the point $P(\theta,\phi)$

(ii) w_n is the complex weight applied across the n^{th} element

(iii) $\vec{g}_n(\theta,\phi)$ is the pattern of the n^{th} element

(iv) $\hat{u}_R$ is the unit vector along the radial line from the array phase-center to P

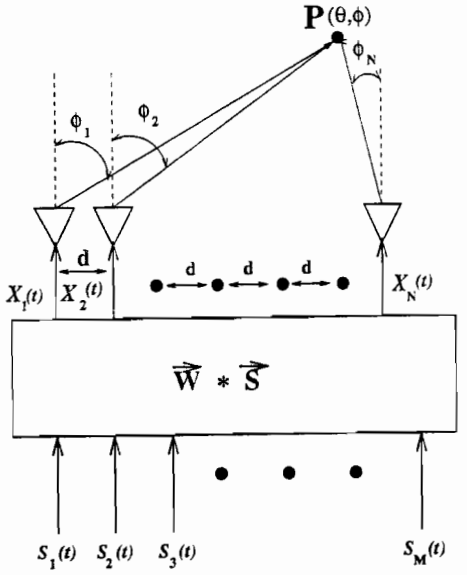

Figure 3.1: General Concept of Digital Beamforming

In (1) the spherical wave factor $\frac{e^{-jk_0 r}}{r}$ has been suppressed. The main objective of pattern synthesis is to determine the set of complex weights w_n for a desired $\left|\vec{E}(\theta,\phi)\right|$.

An adaptive antenna array is one which continuously adjusts (or adapts) to the environment by changing the w_n to obtain desired pattern control. Essentially this feature also contributes to the diversity performance in smart antennas for CDMA applications [8-10]. Various optimization techniques [11] can be employed to determine the weights in (1). For Rapidly Deployable Radio Network systems it is necessary that the transmitting (or base-station) antennas be capable for 360° beamsteering in the azimuth and arbitrary pattern control. Therefore it is necessary to design and implement algorithms that can accomplish this task.

The $\vec{g}_n(\theta,\phi)$ is the radiating pattern of the individual radiating element. This contains information about the mutual reactions between neighboring elements. If mutual coupling is ignored (or assumed to be the same for each element) then one can rewrite (3.1) as

$$\vec{\mathbf{E}}(\theta,\phi) = \vec{\mathbf{g}}_a(\theta,\phi) \times \mathcal{F}_{array}(\theta,\phi) \tag{3.2}$$

where

$$\mathcal{F}_{array}(\theta,\phi) = \sum_{n=1}^{N} w_n e^{j k_0 \hat{\mathbf{u}}_R \cdot \vec{r}_n}. \tag{3.3}$$

The specific element geometry and the environment information is contained in the "average" element-pattern $\vec{g}_a(\theta,\phi)$, while the pattern control information is contained in the array factor $F_{array}(\theta,\phi)$. Equation 4.3 is also known as "beamforming" equation, since it dictates the overall array eprformance. For most practical antenna elements $\vec{g}_a(\theta,\phi)$ is a slowly varying quantity. It therefore follows from 3.2 that 3.3 primarily dictates the overall array performance. Interestingly, 4.3 can be treated separately from the electromagnetic phenomena associated with radiation from antennas. This is a feature that allows much simplification in developing beamforming algorithms without bothering about the design of the actual antenna.

The major limitation in applying 3.2 is that the array has to be fairly large in physical size for 3.2 to be valid [5-7]. Physically large antenna arrays are not easily deployable. Consequently one has to resort to the original equation (3.1) for a more accurate characterization of the array performance. Indeed 3.1 can be employed in place of 3.3 for development of beamforming algorithms. However, for that purpose the individual (or a reasonable subset of) element patterns, $\vec{g}_n(\theta,\phi)$, need to be computed or measured a-priori [5, 11-13]. The necessity of knowing the individual radiating elements do not "see" the same radiating environment as in an infinitely large array, which is the bases of 3.2.

Despite all these limitations, 3.3 is still used to develop beamforming algorithms. Once the w_n are determined and $\vec{g}_n(\theta,\phi)$ are known, it is simple to predict the array performance via 3.1. The various $\vec{g}_n(\theta,\phi)$ are normally computed *ignoring* mutual coupling and the computations are validated by a power pattern measurement as reported in [19]. It appears that this is a cost-effective approach in obtaining the $\vec{g}_n(\theta,\phi)$.

Referring to Figure 3.1, one can write

$$\begin{bmatrix} X_1 \\ X_2 \\ \vdots \\ X_N \end{bmatrix} = \begin{bmatrix} w_{11} & \cdots & w_{1M} \\ w_{21} & \cdots & w_{2M} \\ \cdots & \ddots & \cdots \\ w_{N1} & \cdots & w_{NM} \end{bmatrix} \cdot \begin{bmatrix} S_1 \\ S_2 \\ \vdots \\ S_M \end{bmatrix}. \tag{3.4}$$

In 3.4 the $S_{m=1,\cdots M}$ are the time-domain signals and $X_{n=1,\cdots N}$ are the weighted signals appearing at the input port of the individual antenna elements. The complex excitations are generally defined by $w_{pq} = M_{pq} e^{J\phi_{pq}}$. In a DBF technique the amplitudes M_{pq} and phases ϕ_{pq} can be controlled independently. The exact mechanism of control is not important for characterizing the array antenna. However, the flexibility of independent control provides increased degress of freedom at the signal level [3]. One notes that pattern control is achieved by changing the various w_{pq}. This means that the amplitude and phase distribution across the array aperture can be changed by controlling the w_{pq}. This in turn provides control over the antenna pattern. It can be established that the resulting array pattern (in space-time domain) is given by

$$\vec{\mathbf{E}}(\vec{\mathbf{r}}, t) = \sum_{m=1}^{M} S_m(t) \sum_{n=1}^{N} w_{nm} \vec{\mathbf{e}}_n(\vec{\mathbf{r}}). \tag{3.5}$$

Equation 3.5 is more general than in [3, Eq. (1a)]. (Its complete derivation and implications shall be furnished in a forthcoming report). From 3.5 one notes that the vector quantitity

$$\vec{\mathbf{F}}(\vec{\mathbf{r}}) = \sum_{n=1}^{N} w_{nm} \vec{\mathbf{e}}_n(\vec{\mathbf{r}}) \tag{3.6}$$

is similar to (1). One may note by comparing 3.1 and 3.6 that

$$\vec{\mathbf{e}}_n(\vec{\mathbf{R}}) = \vec{\mathbf{g}}_n(\theta, \phi) e^{\jmath k_0 \hat{\mathbf{u}}_R \cdot \vec{\mathbf{r}}_n} \tag{3.7}$$

This basically establishes the relationship between the DBF concept and conventional array theory. As a consequence the conventional array design and analysis techniques are therefore applicable. To characterize a DBF array, the conventional array synthesis techniques are employed to determine the excitation weights for a prescribed set of pattern constraints. However, all radiators are mounted on structures and they may affect the performance of the antenna array. To account for the structural effects, one needs to include the interaction of electromagnetic radiation from the array and the support structure. This is described in [5] and [14] and is summarized below.

3.3 Uniform Theory of Diffraction

The Uniform Theory of diffraction (UTD) [14] is a high-frequency asymptotic technique for analyzing interactions between complex structures and an antenna. This is the most useful

way to consider path losses in mobile environments [16-18]. Indeed in [16] the r.m.s delay spread is computed for non line-of-sight ray paths using this technique in cellular environment.

The key to the success of the UTD is the fact that a complicated structure is a composition from many simple structures such as wedges, cylinders, spheres and thin plates. When an electromagnetic wave strikes an object, then one can visualize such a process via the conventional ray-theory. To that end, diffracted rays like reflected rays are also generated. The diffracted field, $\vec{E}^d$, along such rays is described by the equation

$$\vec{\mathrm{E}}^d = \vec{\mathrm{E}}^i \cdot \overline{\overline{\mathrm{D}}} A(s) e^{-jk_0 s}. \tag{3.8}$$

In the above

(i) $\vec{E}^i$, is the incident field striking the object
(ii) $\overline{\overline{D}}$ is the dyadic diffraction coefficient
(iii) $A(s)$ is the amplitude spreading factor
(iv) s is the appropriate ray path from source to receiver

For determining the reflected field, $\vec{E}^d$, (8) is used with the appropriate dyadic reflection coefficient $\overline{\overline{R}}$ [14]. Some of the dominant ray paths employed in most UTD calculations

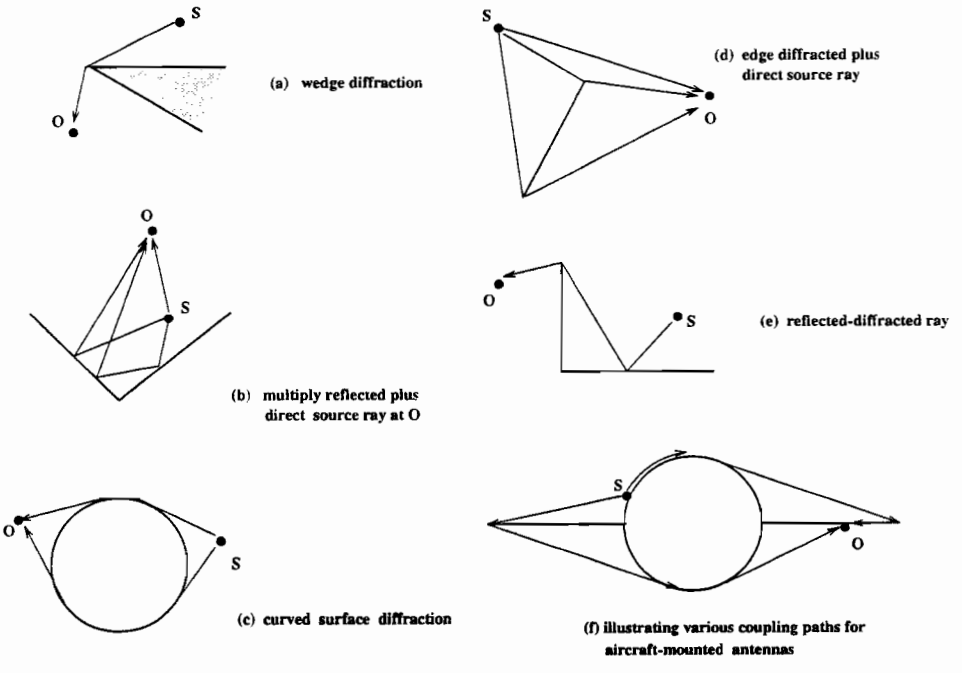

Figure 3.2: Illustrating various ray paths employed in the quasi-optic formulations in NEC-Basic Scattering Code (NEC-BSC). Here S and O are the source and observer locations, respectively.

[14, 15, 17] are shown in fig. 3.2. The laws of ray-optics are employed to find out the ray paths. The dyadic diffraction (or reflection) coefficient in 3.8 is specific for each type of canonical geometry and includes polarization effects. The diffraction (or reflection) coefficient is derived by starting with the exact, dyadic Green's function of the appropriate boundary value problem [14]. The theory in [14] is available in the form of a commercially available computer software known as the NEC-Basic Scattering Code (NEC-BSC) [15].

In the NEC-BSC a complicated structure is defined in terms of several canonical geometries. (these have to be defined by the user following the instructions in the user's manual [15]). The antennas are defined by their complex excitation weights, dimensions, and relative locations with respect to the structure or scattering object. Once these are defined, then the code [15] will decide which ray paths are the most significant for a pair of source and observer locations. The field along these ray paths are computed according to the appropriate formulation that is internal to the code and is opaque from the user. There is a shadowing algorithm internal to the NEC-BSC code which decides the categories of ray paths that will reach the receiver. For modeling the r.f. propagation path in a mobile cellular environment [16-18], the ray paths shall change depending on the channel topology for a pair of source and observer locations. (In [2] the NEC-BSC formulations have been validated by comparing them against exact results for the same canonical problem.) This defines the fast or slow fading due to diffracted and other categories of rays, illustrated in Fig. 3.2.

The field $\vec{E}_p$ along the p^{th} ray path is computed according to the appropriate formulations in [15]. The field from the various paths are then superposed vectorially to find the total field $\vec{E}_{total}$. For computing the r.f. propagation path loss, it is sometimes necessary to compute the Friis coupling gain [6] in term sof the open-circuit voltage V_{oc} at the receiver antenna. Note that V_{oc} automatically takes into account the polarization mismatch between the receiver and the total field $\vec{E}_{total}$. From [6, p. 302] one finds

$$V_{oc} = \vec{h} \cdot \vec{E}_{total} = \sum_{p=1}^{P} \vec{h} \cdot \vec{E}_p \tag{3.9}$$

where $\vec{h}$ is the effective antenna length and can be obtained from the far-field pattern of the receiving antenna, when it is operating in the transmitting mode [4, 6]. In 3.9 it is assumed that the total number of significant ray paths is P. The Friis coupling gain can then be computed via

$$C_F = \frac{\left| I_r V_{oc} \right|^2}{16 P_r P_t} \tag{3.10}$$

All these are internal to the code, opaque from the user. It is emphasized that far-field patterns of an antenna including the structural effects can be computed depending on the user-defined input data. Thus, if the antenna excitation weights are known, the NEC-BSC can be used to include

the radiation effects in the presence of appropriate structures. In 3.10 P_t and P_r are the total radiated powers by the transmitting and receiving antennas, respectively. (These have to be supplied by the user.) Multiple source and receive antennas can also be handled by the NEC-BSC. Due to the mathematical nature of the formulation, the results from the NEC-BSC are expected to be more accurate as the frequency is increased.

Therefore, once the excitation eights of the appropriate elements in an array are determined the effects of the antenna structure can be taken into account. This implies that the linear array with its support structure and an array of dipoles around a cylinder can be modeled effectively via the NEC-BSC. The linear array is described next followed by the conformal cylindrical array.

3.4 Eight Element Linear Array

Fig. 3 illustrates the linear array geometry while the corresponding radiation patterns are shown in Figs. 4 and 5. The array patterns were computed by taking into account the effects of the support structure in Fig. 3.

The linear array was used with the extreme elements unexcited (parasitic). Only elements #2 to #6 were excited. For beamsteering to a predefined angle Φ in the azimuth, the successive excitation phases φ_m were computed from [7, p. 282]: $\varphi = \frac{2\pi d}{\lambda}$. Then the individual excitation phases are $m\varphi$, where $m = 0,12,\cdots$. The excitation was expressed as $1.0e^{jm\varphi}$. For the result in Fig. 5 the complex excitations used in both measurement and computations were:

$$1e^{j0^0}(\#2), 1e^{j45.0^0}(\#3), 1e^{j90.0^0}(\#4), 1e^{j135.0^0}(\#5), 1e^{j180.0^0}(\#6), 1e^{j225.0^0}(\#7).$$

It is to be remembered that elements #1 and #8 were unexcited (parasitic). Once the excitation

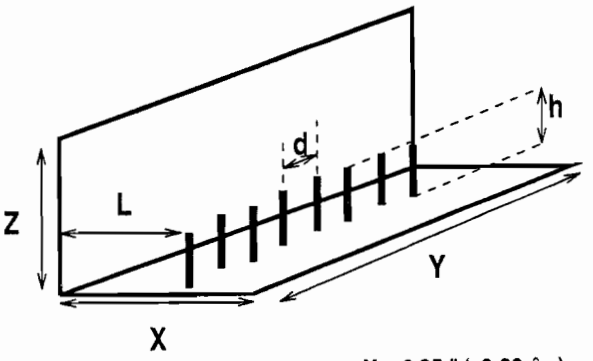

X = 6.25 " (0.66 λ)

f = 1.25 GHz (λ = 9.5 ")

Y = 39.5 " (4.16 λ)

h = 2.125 "(0.224 λ)

Z = 6.25 " (0.66 λ)

d = 4.75 " (0.5 λ)

L = 3.0 " (0.316 λ)

Figure 3.3: The eight element monopole array and its mounting structure

Phases were defined, the geometry of the support structure was also considered as input to the NEC-BSC. Additionally, the ground was also included in the input model. Referring to Fig. 4 one can notice that there is generally good agreement between the measured and computed patterns near the mainbeam region. In Fig. 3.5 a comparison is provided for a 15° beam shift from the boresight. The antenna support structure and the ground were taken into consideration in the calculations. The results indicate that the model is quite accurate near the mainbeam region. Again, the measured and computed patterns show good agreement near the mainbeam region. At $\Phi = -60°$ in both these figures there is a large discrepancy which is due to the fact that there was a strong scattering object whose effects could not be taken into the model.

In general this comparison verifies the performanced of the antenna array and beamsteering and the hardware implementation of the DBF technique.

3.5 Conformal Cylindrical Array

The discussion on the conformal array is summarized from [2]. To determine the complex excitation weights w_n it was found that an amplitude and phase taper were necessary. The main problem was that such amplitude and phase tapers are used for linear arrays [4]. There exists no simple design approach to determining the excitation weights for the conformal cy lindrical array. This was one of the first challenges that had to be solved.

This was accomplished as shown in Fig. 3.6. The conceptual detials of arriving at Fig. 3.6 are included in [2] and are omitted here for brevity. As shown in Fig. 3.6, even-symmetric phase and amplitude distributions were sampled non-uniformly across the projected arch length. It has been shown in [2] that the additional parabolic phase taper provided further improvements in pattern control. In Fig. 3.7 a proposed geometry for realizing a conformal microstrip array is shown. It is evident that the array size decreases as the frequency is increased.

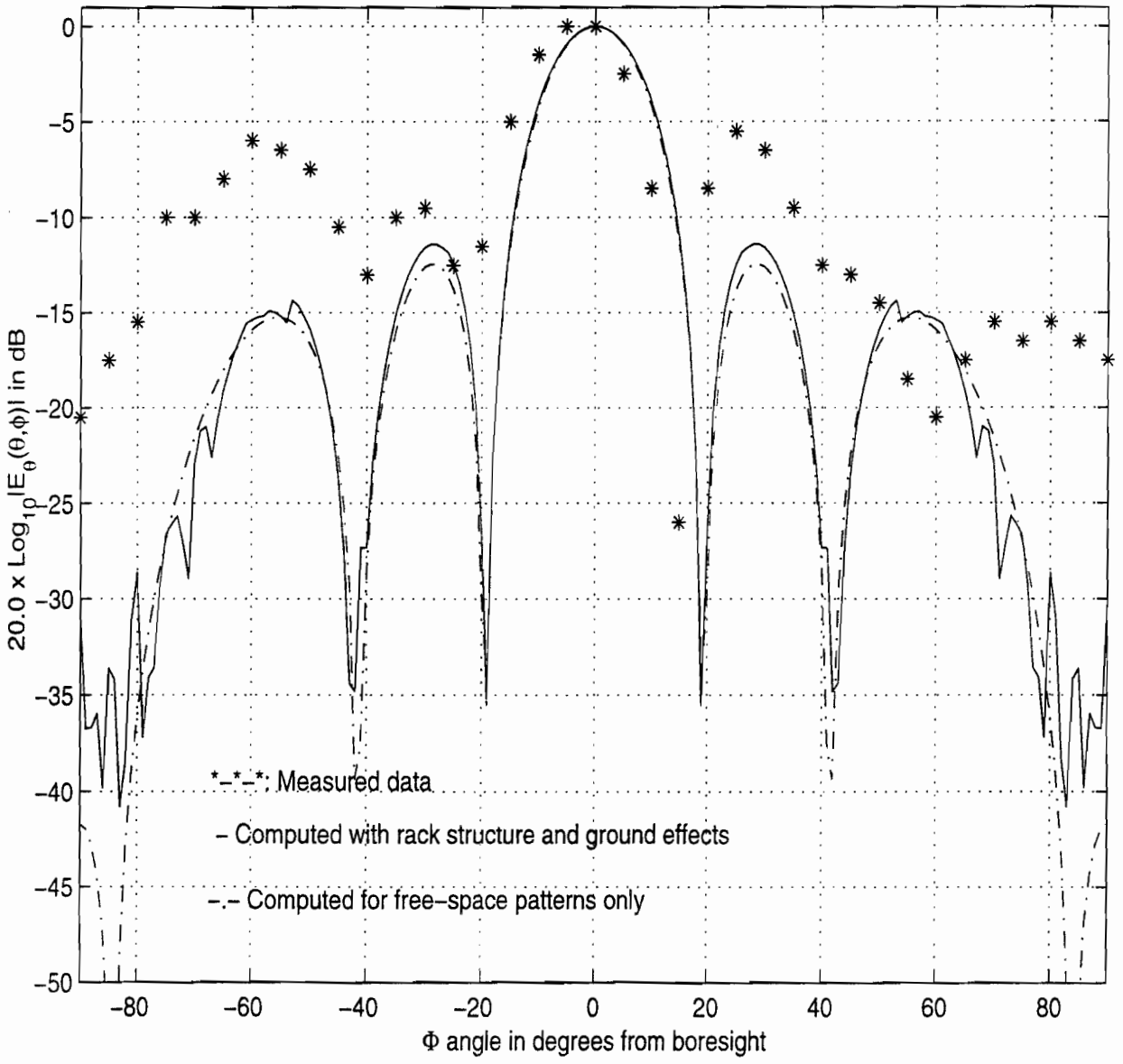

Figure 3.4: Comparison of measured and computed patterns at boresight

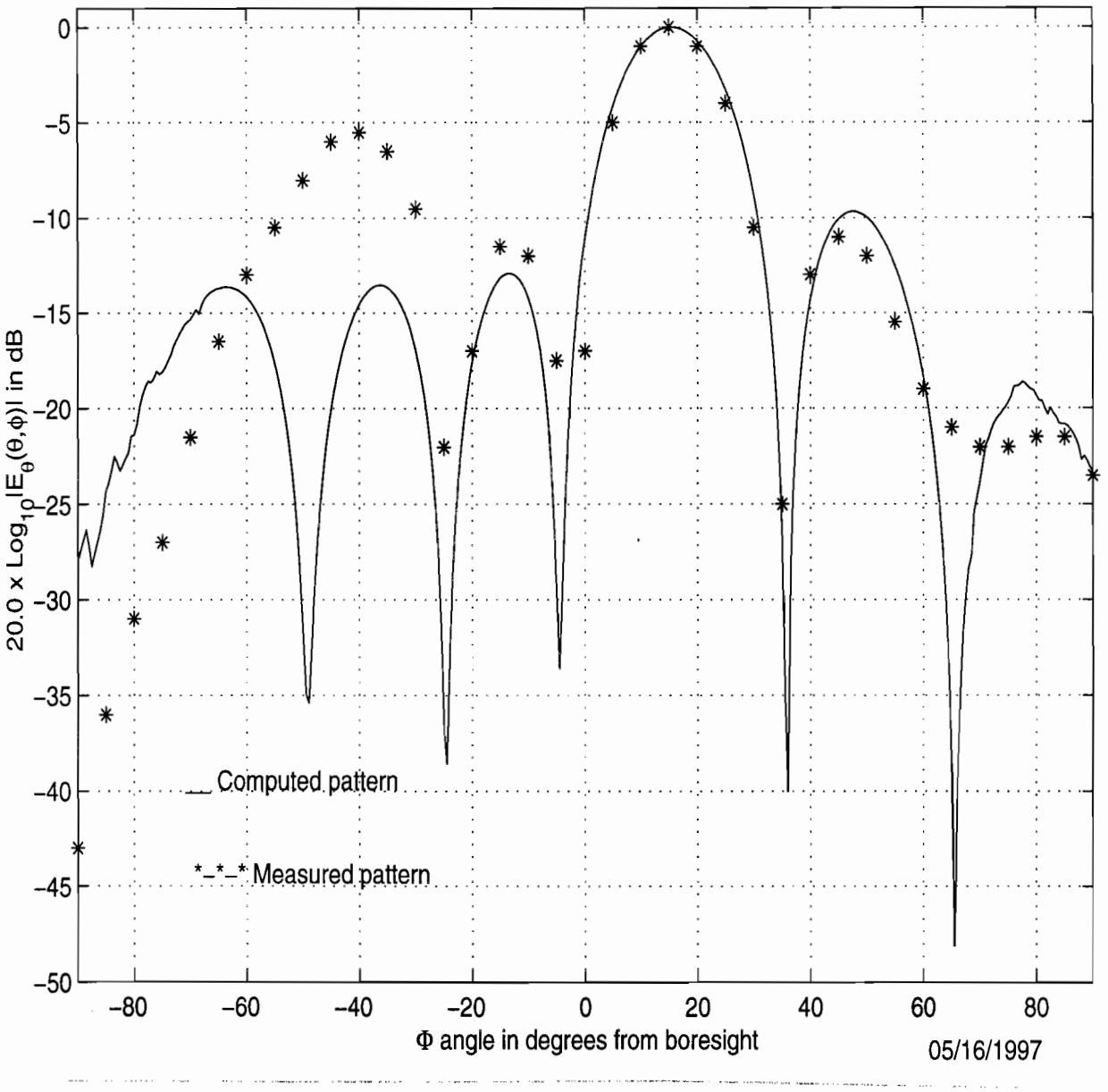

Figure 3.5: Comparison of measured and computed patterns at 15° from boresight

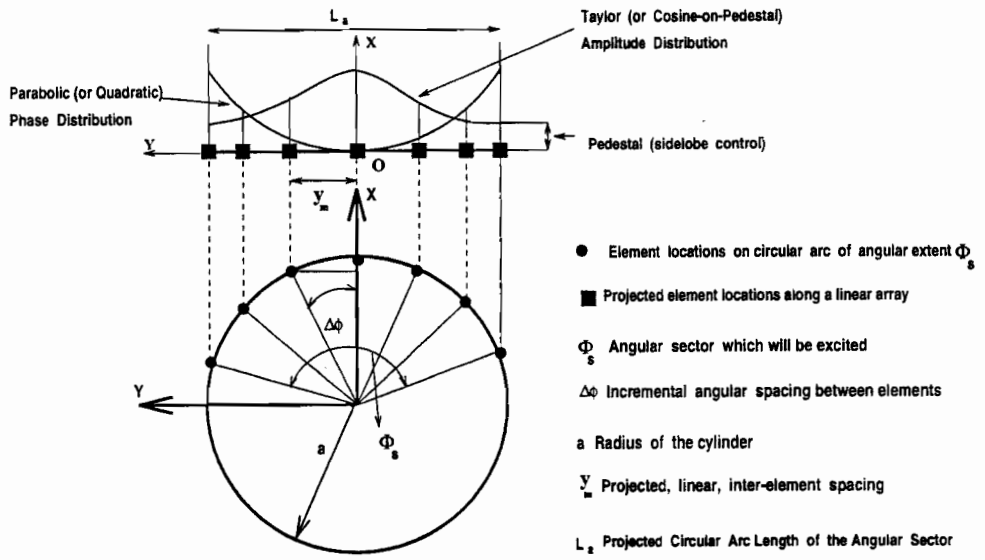

Figure 3.6: Illustrating the basic concept involved in obtaining improved pattern control for cylindrical arrays

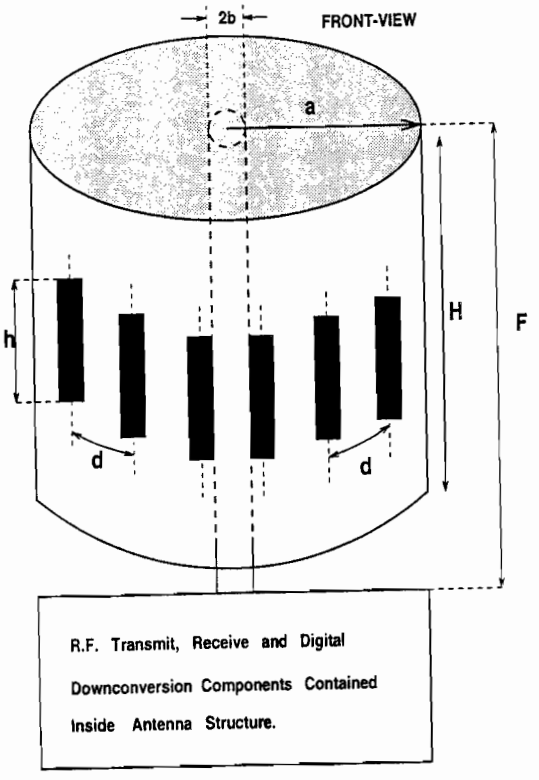

@ 1.25 GHz

λ = 9.5 " (24 cms)
h = 3.62 " (0.38 λ)
d = 5.3 " (0.55 λ)
H = 31.7 " (3.55 λ)
a = 25. 8 " (2.7 λ)

@ 5.8 GHz

λ = 2.04 " (5.2 cms)
h = 0.78 " (0.38 λ)
d = 1.06 " (0.52 λ)
H= 7.3 (3.55λ)
a = 2.68 " (1.313λ)

Figure 3.7: Geometry of a Conformal Microstrip Array of Axial Electric Dipoles

PARAMETERS	ARRAY # 1	ARRAY # 2
Frequency	5.8 GHz	5.8 GHz
Total Number of Elements	18	301
Cylinder Radius	0.0658 m (1.273λ)	1.3608 m (26.33λ)
Angular Sector of Excitation	124.14^0	33.6^0
Number of Elements excited in the sector	7	29
Inter-element Spacing	0.55λ	0.55λ
Amplitude Taper ($\bar{n}$=8 ; SLL=-70 dB)	Taylor	Taylor
Phase Taper	Parabolic	Parabolic
3-dB Beamwidth	40 degrees	6 degrees
1st Sidelobe Level	-30 dB	-16 dB

Figure 3.8: Comparison of performance of two conformal cylindrical arrays at f = 5.8GHz.

In Figures 3.8 and 3.9 a comparison is provided for electrically larger cylinders. The results in Figure 3.8 show that the narrower beamwidths can be obtained with electrically larger cylinders at the expense of higher sidelobe-levels. However, as shown in [2] there is no meaningful beamforming without the amplitude and phase tapers for relatively smaller cylinders.

3.6 **Present and Future Work**

- A conformal cylindrical microstrip patch array comprising of probe-fed, rectangular microstrip patches will be built to operate at 5.8 GHz.
- The algorithm in [2] will be tested on this array. That is, measured patterns will be obtained for comparison against theoretically predicted results.
- The creation of the cylindrical microstrip array analysis code, that will include the actual antenna geometry, has been initiated.

3.7 **Summary**

In this report a brief description of the linear and conformal cylindrical array is presented. The digital beamforming concept has been introduced. The measured and computed patterns for a linear array have been shown to agree reasonably well near the mainbeam region. Some preliminary information for the conformal cylindrical array are also included here. A brief description of the present and future work for RDRN-II has also been included.

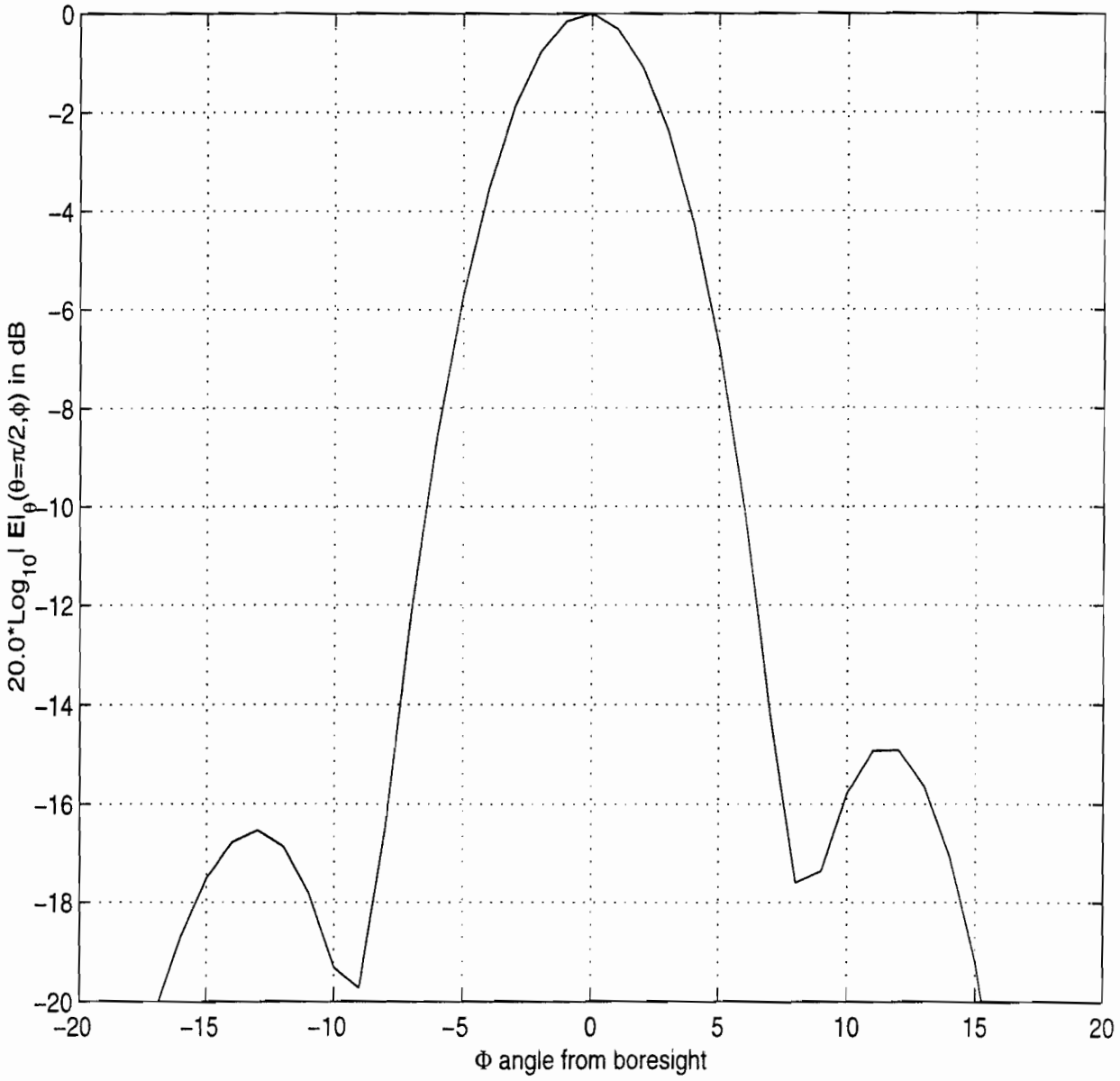

Figure 3.9: Computed far-field pattern of a conformal cylindrical array for $a = 26.33\lambda$

3.8 Bibliography

[1] B. Ewy *et al.*, "An Overview of the Rapidly Deployable Radio Network Proof of Concept system," technical report TISL-10920-16, Information and Telecommunication Technology Center (ITTC), The University of Kansas Center for Research, Inc., Lawrence, Kansas, May 1996.

[2] D. Chatterjee and R.G. Plumb, "Numerical Modeling of Antenna Arrays for Rapidly Deployable Radio networks (RDRN), Part I: Far-Field Patterns of a Cylindrical Conformal Array of Axial Electric Dipoles," Technical Report TISL-10920-14, Information and Telecommunication Technology center (ITTC), The University of Kansas Center for Research, Inc., Lawrence, Kansas, May 1996.

[3] H. Steyskal, "Digital Beamforming at Rome Laboratory," *Microwave Journal*, pp. 100-126, February 1996.

[4] R. A. Sainati, *CAD of Microstrip Antennas for Wireless Applications*, Artech House, Boston, 1996.

[5] W.L. Stutzman and G.A. Thiele, *Antenna Theory and Design*, John Wiley and Sons, NY, 1981.

[6] R.E. Collin, *Antennas and Radiowave Propagation,* McGraw-Hill book Company, NY, USA, 1985.

[7] M.I. Skolnik, *Introduction to Radar Systems,* McGraw-Hill Book Company, NY, USA, 1980.

[8] J.S. Thompson and P.M. Grant and B. Mulgrew, "Smart Antennas for CDMA Systems," *IEEE Personal Communications*, pp. 16-25, October 1996.

[9] A. Naguib, A. Paulraj and T. Kailath, "Capacity Improvement with Base-Station Antenna Arrays in Cellular CDMA," *IEEE Trans. Veh. Technol.*, vol. 43, no. 3, pp. 691-698, August 1994.

[10] S.C. Swales, M.A. Beach, D.J. Edwards and J.P. McGeehan, "The Performance Enhancement of Multibeam Adaptive Base-Station Antennas for Cellular Land Mobile Radio Systems," *IEEE Trans. Veh. Technol.*, vol. 39, no. 1, pp. 56-67, February 1990.

[11] C-Y Tseng and L.J. Griffiths, "A Simple Algorithm to Achieve Desired patterns for Arbitrary Arrays," *IEEE Trans. Signal Process.*, vol. 40, no. 11, pp. 2737-2746, November 1992.

[12] D.F. Kelly and W.L. Stutzman, "Array Antenna pattern Modeling Methods that Include Mutual Couplint Effects," *IEEE Trans. Antennas. Propagat.*, vol. 41, no. 12, pp. 1625-1634, December 1993.

[13] H. Steyskal and J.S. herd, "Mutual Coupling Compensation in Small Array Antennas," *IEEE Trans. Antennas Propagat.*, vol. 38, no. 12, pp. 1971-1975, Dec. 1990.

[14] P.H. Pathak, "High Frequency Techniques for Antenna Analysis," (invited paper), *Proc. Of IEEE,* vol. 80, no. 1, pp. 44-65, January 1992.

[15] R.J. Marhefka and J.W. Silvestro, "Near Zone-Basic Scattering code User's Manual with Space-Station Applications," technical report 716199-13, ElectroScience laboratory, Department of Electrical Engineering, The Ohio State University, Columbus, Ohio, march 1989.

[16] M.C. Lawton and J.P. McGeehan, "The Application of a Deterministic Ray Launching Algorithm for the prediction of Radio Channel Characteristics in Small-Cell Environments," *IEEE Trans. Veh. Technol.*, vol. 43, no. 4, pp. 955-969, November 1994.

[17] W. Zhang, "A Wide-Band Propagation Model Based on UTD for Cellular Mobile Radio Communications," *IEEE Trans. Antennas and Propagat.*, vol. 45, no. 11, pp. 1669-1678, Nov. 1997.

[18] S.Y. Tan and H.S. Tan, "UTD Propagation Model in an Urban Street Scene for Microcellular Communications," *IEEE Trans. Electromagnetic Compatibility,* vol. 35, no. 4, pp. 423-428, November 1993.

[19] D. Loffler, F. Rostan and W. Weisbeck, "Conformal Microstrip Patch Array for SDMA Applications," *IEEE Antennas and Prop. And URSI/USNC Symp.*, vol. 3, pp. 1533-1536, Montreal, Quebec, Canada, July 13-18, 1997.

[20] D. Chatterjee and R.G. Plumb, "Modeling Far Field Patterns of Cylindrical Arrays for Rapidly Deployable Radio Networks (RDRN) Using the NEC-Basic Scattering Code, *IEEE Antennas and Prop. And URSI/USNC Symp.*, vol. 1, pp. 714-717, Baltimore, MD, July 21-26, 1996.

[21] D. Chatterjee and R.G. Plumb, "Comparison of Antenna Architectures for Rapidly Deployable Radio networks (RDRN) based on Far-Field Pattern Performance," *IEEE Antennas and Prop. And URSI/USNC Symp.*, (URSI Abstract Digest), p. 325, Baltimore, MD, July 21-26, 1996.

[22] D. Chatterjee and R.G. Plumb, "Performance Analysis of a Class of Cylindrical Conformal Array Antennas," *IEEE Antennas and Prop. URSI/USNC Symp.*, (URSI Abstract Digest), p. 50, Montreal, Quebec, Canada, July 113-18, 997.

4. RDRN - LINK BUDGET ANALYSIS AND RESULTS

4.1 Introduction

This section of the report gives a summary of the link budget for the Rapidly Deployable Radio Network (RDRN) initial prototype test. A single point-to-point radio link is considered over several paths ranging in distance of up to 10 km. Although the basic link parameters have been specified, the key unknown at this stage is the propagation characteristics of the channel. Therefore, the link budget was done assuming several channel models from the best case of the additive white Gaussian noise (AWGN) channel to the worst case of the Rayleigh fading channel. An outage probability analysis has also been done for the RDRN test link. Measurements from the actual tests conducted with the RDRN prototype have been compared with the results from the test link budget.

From the results of the test link budget it has been established that fading mitigation techniques might be required in the worst case assumption of a Rayleigh fading channel. A particular coding and interleaving scheme considered for RDRN resulted in excessive delay and memory requirements. Therefore, diversity combining along with coding was considered as an option.

Section 2 of this part lists the RDRN prototype system parameters and assumptions. Section 3 summarizes the link budget equations and results. Section 4 explains the results of the outage probability analysis. The initial test measurements and results are given in section 5. The results from packet diversity and coding are summarized in section 6. Section 7 summarizes the results and conclusions.

4.2 RDRN Prototype System Parameters

The RDRN prototype system has the following communication parameter requirements:

- Data rate (r_d) of 1.0 Mbps of uncoded BPSK and coded QPSK and 2.0 Mbps for uncoded QPSK
- Operating frequency range of 1.24 to 1.30 GHz, with a center transmit frequency of 1.27 Ghz
- Communication range (d) of 10 km
- Bit error rate (BER) requirement of 10^{-5}
- 8 element adaptive antenna array for the transmit antenna with a gain of approximately G_t = 10 dB for one steered beam
- Isotropic receive antenna with gain G_r = 0 dB
- Transmit power (p_t) of 680 mW per element yielding 5.44 W

- Receiver noise figure of 5 dB
- Modem implementation loss (L_I) loss of 1.0 dB
- Transmit antenna height of 54 m and receive antenna height of 2 m

4.3 RDRN Test Link Budget

The test link budget was done to obtain the transmit power that would be required to achieve the BER requirement. Since the exact path characteristics between the transmitter and the receiver were not known, three different path models, namely the free-space model, the two-ray model and the Okumura model were considered for the link budget. The free-space model gives us the ideal case situation whereas the two-ray and the Okumura model predicts the path based on practically observation. And four different channels have been assumed for the link budget, namely the AWGN channel, K = 12 dB Rician fading channel, K = 6 dB Rician fading channel, and Rayleigh fading channel. The K = 6 dB and K = 12 dB Rician fading channels are the most commonly observed fading channels for a LOS link, like the one we have for RDRN initial prototype. The required transmit power can be determined by equating the available and the required carrier to noise density ratios as

$$P_t = R_d + \left(\frac{E_b}{N_o}\right)_{req} + L_l - G_t + L_s - G_r + N_o + M_f \qquad (1)$$

where the link budget parameters are

- Data rate (R_d) is 60 dB
- $(E_b/N_O)_{req}$ for BPSK and a BER of 10^{-5} in AWGN is 9.6 dB
- N_0 is the composite noise density of -197.98 dB
- L_S is the path loss
  - For free-space model, L_S is 114.52 dB
  - For two-ray model, L_S is 119.33 dB
  - For Okumura model, L_S is 133.65 dB
- M_f is the fade margin, which is 34.38 dB for the Rayleigh fading, 24.4 dB for the K = 6 dB Rician fading channel and 3.9 dB for the K = 12 dB Rician fading channel.

Tables 1, 2, and 3 tabulate the required transmit power and the link margin for each of the channels assumed and for the different path models assumed. It can be observed that the link does not close for the Rayleigh fading channel for any of the path models and for the K = 6 dB Rician fading channel for the conservative Okumura path model. More details about the RDRN test link budget can be found in [1].

Table 1: Link budget results for the free-space path model

CHANNEL MODEL	TRANSMIT POWER REQUIRED	LINK MARGIN
AWGN	5.176 mW	30.22 dB
Rice K = 12 dB	12.706 mW	26.32 dB
Rice K = 6 dB	1.4256 W	5.82 dB
Rayleigh	14.191 W	-4.16 dB

Table 2: Link budget results for the two-ray path model

CHANNEL MODEL	TRANSMIT POWER REQUIRED	LINK MARGIN
AWGN	15.667 mW	25.41 dB
Rice K = 12 dB	38.459 mW	21.52 dB
Rice K = 6 dB	4.3152 W	1.01 dB
Rayleigh	42.95 W	-8.97 dB

Table 3: Link budget results for the Okumura path model

CHANNEL MODEL	TRANSMIT POWER REQUIRED	LINK MARGIN
AWGN	0.4236 W	11.09 dB
Rice K = 12 dB	1.039 W	7.19 dB
Rice K = 6 dB	116.68 W	-13.31 dB
Rayleigh	1161.44 W	-23.29 dB

4.4 Outage Probability Analysis

For fading channels, BER is not the only performance parameter. The outage probability is a parameter which gives the probability that the link bit error rate will remain below a threshold bit error rate. The following steps are used for calculating the outage probability

- From the link budget, calculate the average SNR by equating the power transmitted to the link budget parameters

$$\bar{\gamma} = P_t - R_d - L_I + G_t + G_r - N_o - L_s = 154.34 - L_s \quad (2)$$

- Use this as the average value to calculate the outage probability for different fading models, i.e., the outage probability value will indicate the probability that the fading signal amplitude is below the threshold value and hence the link will remain closed. The threshold SNR, γ_{thr}, will be 9.6 dB for the required BER of 10^{-5} for BPSK in AWGN.

For Rayleigh fading, irrespective of the modulation scheme employed, the outage probability is given by [2]

$$\Pr(\gamma \le \gamma_{thr}) = P_o = 1 - e^{\frac{-\gamma_{thr}}{\bar{\gamma}}} \quad (3)$$

and for Rician fading it is given by [2]

$$\Pr(\gamma \le \gamma_{thr}) = P_o = 1 - Q\left(\sqrt{(2K)}, \sqrt{\frac{2(1+K)\gamma_{thr}}{\bar{\gamma}}}\right) \quad (4)$$

The link reliability can then be defined as $(1 - P_O)$. Table 4 lists the link reliability for the RDRN test link for various path and channel models. As can be expected, the conservative Okumura path model has low link reliability values.

Table 4: Link reliability for the RDRN test link for various channel and path models

CHANNEL MODEL	FREE-SPACE MODEL	TWO-RAY MODEL	OKUMURA MODEL
Rayleigh	99.91	99.7	92.5
Rice K = 6 dB	99.991	99.97	98.8
Rice K = 12 dB	99.9999997	99.9999991	99.998
AWGN	100	100	100

4.5 RDRN Initial Test Measurements

Several tests were conducted with the RDRN prototype system. The parameters obtained from these tests are as follows:

- The distance between the transmitter and the receiver was approximately 7 km
- The transmit power in the four antenna elements were 2.4 W, 2.55 W, 2.65 W and 2.65 W, summing to a total of 10.25 W
- The received power level was observed to be -67 dBm or -97 dBW (-50 dBm and a -17 dBm receiver gain)
- The 4 element transmit antenna gain was 10 dB

From the test link budget system parameters, the received signal level (RSL) can be predicted as

$$RSL = P_t + G_t - L_s + G_r = 19.11 - L_s \quad (5)$$

Table 5: Predicted received signal levels from the RDRN test link budget

PATH MODEL	PATH LOSS	PREDICTED RSL
Free-space	111.42 dB	-91.31 dBW
Two-ray	113.14 dB	-95.03 dBW
Okumura	129.45 dB	-109.24 dBW

Table 5 lists the predicted received signal level for the various path models. It can be observed that the predicted signal level from the two-ray path model approximately matches that of the actual measured received signal level. Since the RDRN initial test link has line-of-sight, Rician fading can be expected.

4.6 Packet Diversity and Coding Results

From the link budget results, we concluded that fading mitigation techniques will be required if a Rayleigh fading channel occurs (meaning no LOS path) and for other reasons like, increased communication range, lower error rate requirements and increased data rate operations. Therefore, a convolutional coding and inter-block interleaving scheme was considered for the RDRN system [3]. It was found that for RDRN system parameters, implementation of the chosen coding and interleaving scheme will result in a delay requirement of almost a quarter of a second per HDLC frame of data and a memory requirement of almost 30000 bits. This delay requirement is excessive even for delay-insensitive traffic like data. Moreover, since RDRN has prioritized traffic, a separate protocol would have to be devised to allow voice packets to be transmitted when data packets are in the process of being interleaved. These difficulties in the implementation of the interleaving scheme lead us to idea of using diversity combining along with coding but without any interleaving.

Maximal ratio combining (MRC) along with the RDRN half rate convolutional code (k = 7) with Viterbi soft decision decoding was considered for analysis. An extensive analysis of packet error rate performance with MRC and convolutional coding was done in [4] for both Rayleigh and Rician fading channels. It was found that for Rayleigh fading channels, when MRC is employed along with convolutional coding, the gain obtained due to coding over diversity combining was marginal. But the gain increased as the diversity order increases. And for Rician fading channels, quad-diversity along with convolutional coding produced enough gain that the packet error rate performance was as good as in an AWGN channel. The gain obtained due to interleaving along with MRC and coding was very marginal. This can be attributed to the fact as the diversity order increases, the summing up of the faded signals (diversity combining) reduces the probability of burst errors occurring thereby leading to a better coder performance.

Therefore, it can be concluded that if RDRN is still assumed to have a LOS fixed path or meaning a Rician fading channel, interleaving is not necessary to mitigate fading. A quad-diversity maximal ratio combining along with convolutional coding will produce enough gain for the link to remain closed. However, future RDRN systems will have mobile users and might not have a LOS path. The fading distribution in such cases most likely will be Rayleigh. The gain produced by using employing quad-diversity combining with convolutional coding will just be enough for the link to close. But if the system parameters are changed, say lower BER requirements or higher data rate, then either the diversity order has to be increased, resulting in implementation difficulties, or a suitable interleaving scheme has to devised taking into consideration the delay requirement and the prioritized traffic in RDRN.

Table 6: Link margin results with quad-diversity and convolutional coding

	Rice K = 12 dB Link margin	Rice K = 6 dB Link margin	Rayleigh Link margin
Free-space path model	34.02 dB	30.82 dB	24.84 dB
Two-ray path model	29.22 dB	26.01 dB	20.03 dB
Okumura path model	14.89 dB	11.69 dB	5.71 dB

Table 6 gives the link margin results when quad-diversity maximal ratio combining is employed along with convolutional coding with soft decision decoding and without interleaving for the RDRN initial prototype system. It can be seen that the RDRN initial test link now closes for all the path models and channel assumptions. However, for Rayleigh fading and the conservative Okumura path model, the link just closes with less link margin.

4.7 Summary of Results and Conclusions

The link budget for the RDRN prototype system was done for three different path models and four different channel models. The link does not close for a Rayleigh fading channel assumption for any of the path models. Also the link does not close with the K = 6 dB Rician fading channel for the conservative Okumura path model. This lead to the conclusion that fading mitigation techniques will be necessary for future RDRN systems.

From the measurements obtained from the initial tests conducted with the RDRN prototype system, we conclude that the path model between the transmitter and the receiver matches a two-ray (fourth power law) model. This was concluded by verifying the predicted received signal level for various path models from the link budget with the measured received signal levels.

A particular coding and interleaving scheme considered for the RDRN system resulted in excessive delay and memory requirements. Therefore, a detailed analysis of the BER and packet error rate performance was conducted when diversity combining is employed with coding instead of interleaving. This analysis lead to the conclusion that quad-diversity maximal ratio combining along with a half-rate convolutional coding with Viterbi soft decision decoding produces enough gain to keep the link closed with a considerable link margin for the Rician fading channels and with just enough link margin for the Rayleigh fading channel. Therefore, it can be concluded that if the system parameters are changed, meaning lower BER requirements or

increased communication range and/or higher data rates, then either the diversity order needs to be increased, resulting in hardware complexities, or a suitable interleaving scheme needs to be devised.

4.8 Bibliography

[1] Vijayanand K. Paulrajan and James A. Roberts, "RDRN - Link Budget," *Technical Report TISL-10920-18, The University of Kansas Center for Research Inc.,* May 1996.

[2] James A. Roberts, "EECS 865 - Class notes," *Department of EECS, University of Kansas,* Aug. 1996.

[3] Vijayanand K. Paulrajan and James A. Roberts, " RDRN - Interleaving Requirements," *Technical Report TISL-10920-25, The University of Kansas Center for Research Inc.,* Jan. 1997.

[4] Vijayanand K. Paulrajan, "Packet communication performance with diversity combining and error correction coding in Rayleigh and Rician fading channels," *Masters thesis, University of Kansas,* Sep. 1997.

5. RDRN ATM INTERNETWORKING DEMONSTRATION

In July 1997, an RDRN testbed was demonstrated at the semi-annual DARPA GLOMO meeting in Long Branch, New Jersey. The setup featured an RDRN network prototype in a minimal configuration (i.e., one Edge Switch (ES) and one Remote Node (RN)). The demonstration has four goals:

1. Demonstrate the orderwire system for network configuration and control,
2. Show integration of RDRN and ATM technologies,
3. Demonstrate end-to-end connectivity over heterogeneous wired and wireless technologies, and
4. Show interoperability with other GLOMO participants and the Internet at large.

Achieving seamless communications over an heterogeneous environment involving wired and wireless technology represents a challenge due to the many differences between such networks. Further, with today's internetworking success in linking computers and users over the Internet, interoperability with legacy networks is crucial. Over the past two years, the Rapidly Deployable Radio Network (RDRN) project has built and deployed an architecture to provide seamless support for communications over an ATM-based wired/wireless networks while still being able to interoperate with legacy IP-based networks. This section presents the results of an exercise to demonstrate the capabilities of the RDRN network indicated above.

Figure 5.1 illustrates the configuration for the internetworking demonstration. The RDRN testbed has been highlighted for clarity purposes. The first three goals are demonstrated within the context of the RDRN testbed alone. The fourth goal extend the overall testbed to include a connection to the USC's WING (Wireless Internet Gateway) ad-hoc network [USC:Wings] and a local Internet Service Provider (ISP).

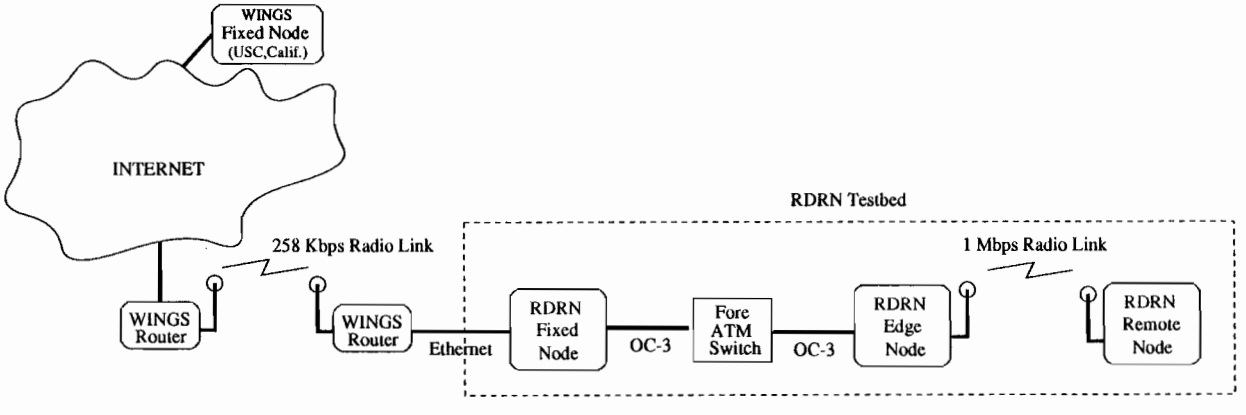

Figure 5.1: RDRN Internetworking Demonstration

The hardware platform used for the RDRN testbed includes four key components:

Fixed Node (FN): Desktop Pentium Dell 120Mhz running Linux 2.0.25 with a PCI ethernet interface and a PCI Efficient Networks 155 Mbps ATM interface.

ATM Switch: Fore ASX200-WG with 12 OC-3 ports.

Edge Switch (ES): Laptop Tecra 700 CT 120Mhz running Linux 2.0.25 with a PCI Efficient Networks 155 Mbps ATM interface, a PCI 2Mbps Wireless ATM interface (developed by UofKansas), a serial connection to a GPS receiver, and a serial connection to a 19.2Kbps packet radio.

Remote Nde (RN): Laptop Tecra 700 CT 120Mhz running Linux 2.0.25 with a PCI 2Mbps Wireless ATM interface, a serial connection to a GPS receiver, and a serial connection to a 19.2Kbps packet radio.

Configuration details for each of the demonstrations presented above are provided next.

5.1 Orderwire System for Network Configuration and Control

This demo shows the Network Configuration and Control (NCP) protocol in operational mode between the Edge Switch (ES) and Remote Node (RN).

First, previously stored GPS time and position information was retrieved from the GPS receivers. The Kantronics packet radios were then used to disseminate the location information between the ES and RN. The ES maintained a table of RN state information and had the information necessary to establish the high-speed link-level connectivity (i.e., a Wireless ATM channel) to the RN.

All relevant information about the NCP protocol was retrieved via SNMP and displayed on a graphical network monitor at each RDRN node. The graphical interface displayed icons for ESs and a RNs and the relative connectivity between them. Connectivity was show as link in a color depending of the actual state of a connection. By clicking on an icon (e.g., node, link) relevant information can be displayed (e.g., number of NCP packets sent, number of NCP packets received, ES state, RN state, etc).

As a further indication of the real time nature of the demo, turning off the packet radio caused the graphical icon representing the RN to turn red.

5.2 Integration of Wired/Wireless ATM Technologies

The RDRN testbed features a wired ATM segment and a wireless ATM segment. The wired segment enables connectivity of a FN in the ATM network, through standard ATM switches, with a software-based ATM switch integrated into the ES. The wireless segment enables connectivity between the ES and one or more RN(s). End-to-end ATM-level connectivity can be setup between the FN and a RN using either Permanent Virtual Circuits (PVCs) or Switched Virtual Circuits (SVCs). Establishment of PVCs in the RDRN testbed are trivial and have to be done manually along the path of a desired ATM connection. SVCs, on the other hand,

are established dynamically by exchanging ATM signaling messages along the desired connection.

The software-based ATM switch integrated into the ES have the capability to understand NNI messages (for connections with other ATM switches) and UNI messages (for connections to directly connected FNs or remotely connected --via wireless-- RNs). For the purpose of the demo, the RN first got assigned an ATM address by the ES using ILMI (once indicated by the orderwire system that link connectivity was required between the ES and RN). Similarly, the FN got assigned an ATM address by the directly connected ATM switch. An SVC connection between the FN and the RN was then established using Classical IP (CLIP) over ATM. For this to work, an ATMARP server was run on the Fore ATM switch and both FN and RN have to registers their ATM address, along with an IP address, with the server. Once the ATM registration at the ATMARP server is done, both FN and RN are capable to talk to each other using their assigned IP addresses (which later gets resolved into the destination ATM address necessary to establish and SVC connection).

5.3 End-to-End Heterogeneous Networking IP over ATM/WATM

As indicated in the previous section, an SVC connection was setup between the RN and the FN using CLIP over ATM. Having each node assigned an IP address, and their routes configured to point to their local ATM interfaces (the RN points to the Wireless-ATM interface) completed the configuration needed to establish end-to-end communication between the two nodes.

Two basic IP-based applications were demonstrated live over the pre-configured SVC between the FN and RN: finger and telnet. In addition, a teleconferencing session using the Mbone tools was setup between the FN and RN. The Mbone session was advertised using the sdr (Session Directory Tool) tool, live audio was sent using the VAT Mbone tool, and video stream was sent using the VIC Mbone tool. In particular, the quality of the video sent averaged a rate of ten to twelve frames per second.

5.4 Interoperability with other GLOMO Participants and the Internet

During the GLOMO meeting, the RDRN testbed was connected with the University of California at Santa Cruz's WINGS (Wireless Internet Gateways) [USC:Wings] network. WINGs is a mobile wireless architecture in which packet-radio nodes are easily-reconfigurable wireless IP routers. The wireless IP routers are designed to enable global IP Internet access to ad-hoc networking environments. Routing in WINGS is accomplished at the IP level, just as its counterpart the IP router, with the addition that the wireless router must also adapt to the dynamics of an ad-hoc network in which the nodes move frequently.

Connecting the RDRN testbed to the WINGs network went smoothly considering that only one day was given to complete the setup. The WINGs network configuration consisted of a multihop network of WINGs routers. Each WINGs router is basically an IP router (running FreeBSD) with a 10baseT line out of the back and a radio on top. The WING that was connected to the FN, through an ethernet hub, served as the border router for the rest of the RDRN testbed.

The overall configuration basically treat the RDRN testbed as a subnet of the major WING network. The WING border router and the FN configured their routing table to learn about the existence of each other. Once this was done, unicast IP packets could be sent from either the FN or RN in the RDRN testbed to any node in the WINGs network and viceversa. Multicast packets could also be sent since the WINGs network acts as a multicast bridge across that domain. Further, since the WINGs network was also connected to a local ISP, connectivity to the Internet at large was available.

In one demonstration, a WWW session was run on the RN for browsing the Internet. In a second demonstration, USC was broadcasting an Mbone live video session from Santa Cruz, California via Internet. The sdr Mbone tool running on the RDRN RN detected the USC's advertisement and displayed the live video using VIC. As an added bonus, USC setup a WWW homepage in which individual users could control the images to be downloaded from the video camera on the USC campus. Therefore, by modifying the direction of the camera via WWW, users could observe different angles of the image displayed by the Mbone VIC tool. Nonetheless, the quality of the video sent averaged a very low rate due to the low channel bit rate featured by the WING routers.

5.5 Bibliography

USC:Wings On-line description available at http://www.cse.ucsc.edu/research/ccrg/projects/wings.html. University of California at Santa Cruz.